AD_____

Award Number: DAMD17-01-1-0029

TITLE: Comprehensive Development Program of Hunter-Killer Peptides for Prostate Cancer

PRINCIPAL INVESTIGATOR: Howard M. Ellerby, Ph.D.

CONTRACTING ORGANIZATION: Buck Institute for Age Research
Novato, California 94948

REPORT DATE: May 2003

TYPE OF REPORT: Annual

PREPARED FOR: U.S. Army Medical Research and Materiel Command
Fort Detrick, Maryland 21702-5012

DISTRIBUTION STATEMENT: Approved for Public Release;
Distribution Unlimited

The views, opinions and/or findings contained in this report are those of the author(s) and should not be construed as an official Department of the Army position, policy or decision unless so designated by other documentation.

20031031 098

REPORT DOCUMENTATION PAGE

Form Approved
OMB No. 074-0188

Public reporting burden for this collection of information is estimated to average 1 hour per response, including the time for reviewing instructions, searching existing data sources, gathering and maintaining the data needed, and completing and reviewing this collection of information. Send comments regarding this burden estimate or any other aspect of this collection of information, including suggestions for reducing this burden to Washington Headquarters Services, Directorate for Information Operations and Reports, 1215 Jefferson Davis Highway, Suite 1204, Arlington, VA 22202-4302, and to the Office of Management and Budget, Paperwork Reduction Project (0704-0188), Washington, DC 20503

1. AGENCY USE ONLY (Leave blank)	2. REPORT DATE May 2003	3. REPORT TYPE AND DATES COVERED Annual (1 May 2002 – 30 Apr 2003)

4. TITLE AND SUBTITLE
Comprehensive Development Program of Hunter-Killer Peptides for Prostate Cancer

5. FUNDING NUMBERS
DAMD17-01-1-0029

6. AUTHOR(S)
Howard M. Ellerby, Ph.D>

7. PERFORMING ORGANIZATION NAME(S) AND ADDRESS(ES)
Buck Institute for Age Research
Novato, California 94948

E-Mail: mellerby@buckcenter.org

8. PERFORMING ORGANIZATION REPORT NUMBER

9. SPONSORING / MONITORING AGENCY NAME(S) AND ADDRESS(ES)
U.S. Army Medical Research and Materiel Command
Fort Detrick, Maryland 21702-5012

10. SPONSORING / MONITORING AGENCY REPORT NUMBER

11. SUPPLEMENTARY NOTES
Original contains color plates: All DTIC reproductions will be in black and white.

12a. DISTRIBUTION / AVAILABILITY STATEMENT
Approved for Public Release; Distribution Unlimited

12b. DISTRIBUTION CODE

13. ABSTRACT (Maximum 200 Words)

Prostate cancer is now the most common cancer among men in the United States. Angiogenesis is required for prostate tumor survival, growth, and metastasis. We proposed to design novel Hunter-Killer Peptides (HKPs), each representing a chimeric peptide of an angiogenesis-targeting peptide and a mitochondrial membrane-disrupting peptide. While *non-toxic* in the circulation, the HKPs will be preferentially *toxic* to mitochondria once internalized into angiogenic cells, via the targeting domain. As we reported in Ellerby *et al.*, *Nature Medicine*, 5, 1032-1038, 1999, our prototypes contain only 21 and 26 amino acid residues, are selectively toxic to angiogenic endothelial cells and show strong anti-cancer activity in mice (breast carcinoma xenografts). In the work described here, we evaluated the HKPs for efficacy and toxicity in a xenograft model of human prostate carcinoma, and in the TRAMP (transgenic adenocarcinoma mouse prostate) model for prostate cancer. The central theme of this research is to develop and appraise this new chemotherapy with the goal of producing both a safer, and more effective, treatment of advanced prostate cancer.

14. SUBJECT TERMS No subject terms provided.	15. NUMBER OF PAGES 57
	16. PRICE CODE

17. SECURITY CLASSIFICATION OF REPORT Unclassified	18. SECURITY CLASSIFICATION OF THIS PAGE Unclassified	19. SECURITY CLASSIFICATION OF ABSTRACT Unclassified	20. LIMITATION OF ABSTRACT Unlimited

NSN 7540-01-280-5500

Standard Form 298 (Rev. 2-89)
Prescribed by ANSI Std. Z39-18
298-102

Table of Contents

Introduction

The subject of our research is prostate cancer. The purpose of this research is the development of a more effective and less toxic treatment for prostate cancer. The currently used chemo-therapeutic agents are drugs with the narrowest therapeutic index in all of medicine. Therefore, effective doses of a wide variety of anti-cancer agents are restricted by their non-selective, highly toxic effect on normal tissues. In response to this, we designed short peptides composed of two functional domains, one a tumor blood vessel 'homing' sequence and the other a programmed cell death-inducing sequence, and synthesized them by basic peptide chemistry. The 'homing' domain was designed to guide the peptide to targeted cells and permit its internalization. The pro-apoptotic domain was designed to be non-toxic outside all cells, but toxic when internalized into just the targeted cells by the disruption of mitochondrial membranes.

Thus our approach was to create non-toxic anticancer peptides, which we named **Hunter-Killer Peptides (HKP)**, designed to only destroy tumor blood vessels while leaving normal blood vessels unharmed. As presented in Ellerby *et al.*, 1999, we succeeded in the development of HKPs, demonstrating that although our 2 prototypes contained only 21 and 26 amino acid residues, they were selectively toxic to angiogenic endothelial cells and had strong anti-cancer activity in mice. Furthermore, in Arap *et al.*, 2002, we showed that HKPs delayed the development of the cancers in prostate cancer-prone transgenic mice (TRAMP mice). Moreover we elaborate on our previous report that HKPs can be given IP (intraperitoneal) in addition to IV (intravenous;tail vein injection in mice), opening up the possibility to administer our peptides more than once a week. A manuscript on this work is now in preparation. We also discuss problems and solutions to those problems encountered this year with our CNGRC-based peptides, involving peptide quality, and receptor expression. We conclude this part of the report with a discussion of a study that we have just begun to treat TRAMP mice that spontaneously get prostate cancer, with a dual therapy designed to attack the prostate tumors blood vessels and the prostate cells as well.

We also review and elaborate on our previous report concerning a new anti-cancer therapy that complements our work on targeted antiangiogenic peptides. We have discovered that certain membrane-disrupting/pore-forming peptides can be quite effective as direct anti-neoplastic agents (directly killing cancer cells). Specifically, we review here, as described in our recent published paper (Ellerby *et al.*, 2003), that a 69 amino acid peptide, **Small Globular Protein (SGP)** can reduce tumor volume (eliminating some tumors), and increase survival, in a xenograft model of human prostate carcinoma. We conclude this report with a discussion of a study that we have just begun to treat TRAMP mice that spontaneously get prostate cancer, with a dual therapy designed to attack both the prostate tumors blood vessels and the prostate cells.

Body

Our work to date in designing, synthesizing, and testing Hunter-Killer Peptides (HKPs), and Small Globular Protein (SGP), is described in the accompanying reprints by Ellerby *et al.*, 1999, and Arap *et al.*, 2002, and in our newly published paper Ellerby *et al.*, 2003, in the appendix. In the following, we re-state the approved **Statement of Work**, and then summarize how we have met our goals so far.

Statement of Work

Task 1, Specific Aim 1, (months 0-18). Optimize the dose of current HKPs in the TRAMP C model.

- Establish human PC3-derived tumor xenografts in nude mice (60 mice).
- Establish murine TRAMP C-derived tumors in C57BL/6 mice (60 mice).
- Treat the mice in 1 and 2 with HKPs to determine optimal doses, and dosing schedule.
- Acquire/breed TRAMP C mice (60 mice).
- Treat the mice in 4 with HKPs, beginning with the optimal doses, and dosing schedule, developed in 3 to refine/confirm the optimal doses, and dosing schedule. Histopathological studies will also be performed, to look for efficacy and side effects.

Task 2, Specific Aim 2, (months 0-24). Design HKPs with improved therapeutic indices.

- Design new HKPs using the guiding principles of anti-mitochondrial peptide chemistry.

Task 3, Specific Aim 3, (months 6-24). Evaluate *in vitro* efficacy and toxicity of new HKPs.

- Evaluate the efficacy of new HKPs in mitochondrial swelling assays,
- Evaluate the efficacy of new HKPs in mitochondrial in tissue culture.
- Use the results of 1 and 2 to find approximate doses and therapeutic indices. HKPs with high therapeutic indices will then be evaluated in TRAMP mice, Specific Aim 4.

Task 4, Specific Aim 4, (months 18-36). Evaluate the *in vivo* efficacy of new HKPs in the TRAMP model of prostate cancer.

- Acquire/breed TRAMP C mice (60 mice).
- Treat the TRAMP C mice with new HKPs to determine optimal doses.
- Treat the TRAMP C with new HKPs to determine dosing schedule.
- Histopathological studies will also be performed, to look for efficacy and side-effects.

Task 5, Specific Aim 5, (months 24-36). Determine the *in vivo* pharmacokinetics of HKPs in the TRAMP model of prostate cancer.

- Acquire/breed TRAMP C mice (60 mice).
- Radiolabel HKPs and treat mice.
- Evaluate tissues, and cells in culture (using our *in vitro* angiogenesis assays, Ellerby *et al.*, 1999), for presence of HKPs. Determine concentrations and locations of HKPs inside cells. Determine concentrations of HKPs in tumor blood vessel endothelial cells. Determine if there are any *in vivo* locations HKPs build up in that might create unwanted side effects.

Summary of Results/Data:

Task 1. As discussed previously, we have established human PC3-derived tumor xenografts in nude mice, and have evaluated the efficacy of SGP (see introduction) in this model (see below and Ellerby *et al.* 2003, for a discussion of these results). Furthermore, we also reported in Arap *et al.*, 2002, that HKPs delayed the development of the cancers in prostate cancer-prone transgenic mice

(TRAMP mice). Thus we are already ahead of schedule on this task, having already demonstrated the efficacy of HKPs in this transgenic mouse model. We have now begun work on the process of optimizing the doses of HKPs in the TRAMP model, and have proceeded to formulate a study in TRAMP mice involving the dual use of HKP's to simultaneously target the angiogenic blood vessels of prostate tumors and the normal prostate cells. This work begins this month. Furthermore, based on these initial results, we plan later this year to also include in some combination with HKP therapy, targeted nanoparticles containing SGP.

Task 2. We are currently designing new HKPs, so this Task is in progress, and will continue throughout the life of these studies. In particular, a new killer sequence has been developed, ALLLAIRRRKKK, based on an antibacterial peptide produced in moths. Initial tests of the efficacy of this peptide in our *in vitro* tissue culture models (see Ellerby et al. 1999), demonstrate that this killing sequence is 1,000-5,000 times more effective than our original killing peptide KLAKLAKKLAKLAK, as measured by the therapeutic index calculated as the ratio of the concentration required to kill normal untargeted cells divided by the concentration required to kill targeted cells. In addition, we have discovered that SGP (see introduction) can be used as a complementary therapy to HKPs. While HKPs target and destroy tumor vasculature, SGP directly kills tumor cells when injected intratumorally. This data is summarized below, and in our recent paper, Ellerby *et al.*, 2003.

Task 3. We are currently testing new HKPs, so this Task is always in progress, and as described above, we have been focusing on HKP's with a new ALLLAIRRRKKK killing domain, for which initial tissue culture studies suggest that this new HKP will be over 1,000 times more effective.

Task 4 and Task 5. These tasks are beginning over the next several months. There was some delay this past year in beginning these studies because we had problems of peptide purity (the peptides are manufactured commercially), and were informed by a colleague that the CNGRC targeting moiety might not be the most optimal targeting peptide to employ, due to variances in receptor expression. This peptide had been selected over more complex targeting peptides such as our ACDCRGDCFC (bicyclic with 2 disulfide bonds) targeting peptide, due to issues involving the cost and complexity of synthesis of the RGD-based targeting peptide. We were fortunate to discover the above before embarking on our complex and expensive TRAMP studies. We will begin our TRAMP study this month using the RGD-based targeting sequence, to target the tumor blood vessels, and the SMS-based targeting sequence (see Arap *et al.*, 2002). In addition, we have been forced by the quality issues to switch to another custom peptide synthesis company.

Key Research Accomplishments

- **We successfully designed and tested a Hunter-Killer Peptide, SMSIARL-GG-$_D$(KLAKLAK)$_2$, in the TRAMP Mouse Model of Prostate Cancer.** *This work is described in Arap et al., 2002, which is attached*

- **We successfully published a paper on our design and evaluation of SGP.** As described above, we successfully tested the anti-tumor effects of SGP in human prostate carcinoma xenografts in nude mice. The data show that SGP can reduce tumor volume and extend survival. *This data is discussed in detail in Ellerby et al., 2003, which is attached.*

- **We worked out issues involving peptide quality (commercial synthesis), and made the decision to switch to a different RGD-based targeting peptide.** We discovered this year after a 3 month study that we were having a problem with the peptide company we dealt with, involving issues about timely delivery and quality of peptide. We also decided to switch to our

RGD-based targeting peptide, in part because some of our *in vitro* tests were inconsistent from peptide batch to peptide batch. This situation was clouded by real concern over quality, but even so, colleagues reported to us that they were just getting a better result with our RGD-based targeting peptide. Thus, in the studies we are about to begin on TRAMP mice, we will be using the RGD-based targeting peptide for HKP's designed to target angiogenic vasculature.

Reportable Outcomes

Papers, manuscripts, abstracts, presentations

(1) Ellerby HM, Arap W, Ellerby LM, Kain R, Andrusiak R, Del Rio G, Krajewski S, Lombardo CR, Rao R, Ruoslahti E, Bredesen DE, Pasqualini R (1999). "Anti-cancer activity of targeted pro-apoptopic peptides." *Nature Medicine* 5(9):1032-1038.

(2) del Rio G, Castro-Obregon S, Rao R, Ellerby HM, Bredesen DE (2001). "APAP, a sequence-pattern recognition approach identifies substance P as a potential apoptotic peptide." *FEBS Lett.* 494(3):213-9.

(3) Arap W, Haedicke W, Bernasconi M, Kain R, Rajotte D, Krajewski S, Ellerby HM, Bredesen DE, Pasqualini R, Ruoslahti E (2002). "Targeting the prostate for destruction through a vascular address." *PNAS* 99(3):1527-31.

(4) Ellerby HM, Lee S, Andrusiak R, Ellerby LM, Chen S, Kiyota T, del Rio G, Sugihara G, Arap W, Bredesen DE & Pasqualini R (2002). "An artificially designed pore-forming protein with anti-tumor effects." In press *J. Biol. Chem.*

Patents and licenses applied for and/or issued

We will be applying for a patent on the use of SGP. This has been reported in the Inventions Report to the DAMD.

Degrees obtained that are supported by this award

None.

Development of cell lines, tissue or serum repositories

None.

Informatics such as databases and animal models, etc

See ref. (2) above by del Rio et al.

Funding applied for based on work supported by this award

None at this time.

Employment or research opportunities applied for and/or received on experiences/training supported by this award

None at this time.

Conclusions

We have designed short peptides, Hunter Killer Peptides (HKP), composed of two functional domains, one a tumor blood vessel 'homing' motif and the other a programmed cell death-inducing sequence, and synthesized them by simple chemistry. The 'homing' domain was designed to guide the peptide to targeted cells and allow internalization. The pro-apoptotic domain was designed to be non-toxic outside cells, but toxic when internalized into targeted cells by the disruption of mitochondrial membranes. We demonstrated in Ellerby *et al.* 1999, that HKPs show strong anti-cancer activity in mice (xenografts of human breast carcinomas and melanomas). We also reported here and in Arap *et al.*, 2002, that HKPs delayed the development of the cancers in prostate cancer-prone transgenic mice (TRAMP mice). The publication of this paper was a milestone for us, and meant that were ahead of schedule with our proposed research (this research was not planned until 2003). Finally, we now have demonstrated the feasibility of using membrane-disrupting/pore-forming peptides/proteins as anti-neoplastic agents by evaluating the efficacy of Small Globular Protein (SGP). This work is being published this month, Ellerby *et al.*, 2003. We now proceed this year to our TRAMP studies, involving the use of HKPs targeted to tumor blood vessels, and HKPs targeted to normal prostate cells. Work will then begin on the consideration of an SGP-targeted therapy, probably involving nanoparticle technology, designed to encase SGP so that it can be injected directly into the blood stream, targeted by a surface coating of targeting peptide. The implications of our work are that it is now possible for humans to engineer targeted and untargeted artificial peptides and proteins to be used systemically and locally as effective anti-cancer agents.

References

Arap W, Pasqualini R, & Ruoslahti E. Cancer treatment by targeted drug delivery to tumor vasculature in a mouse model. *Science* **279**:377-380 (1998).

Arap W, Haedicke W, Bernasconi M, Kain R, Rajotte D, Krajewski S, Ellerby HM, Bredesen DE, Pasqualini R, Ruoslahti E (2002). Targeting the prostate for destruction through a vascular address. *PNAS* 99(3):1527-31.

del Rio G, Castro-Obregon S, Rao R, Ellerby HM, Bredesen DE (2001). APAP, a sequence-pattern recognition approach identifies substance P as a potential apoptotic peptide. *FEBS Lett.* 494(3):213-9.

Ellerby HM, Arap W, Ellerby LM, Kain R, Andrusiak R, Del Rio G, Krajewski S, Lombardo CR, Rao R, Ruoslahti E, Bredesen DE, Pasqualini R (1999). Anti-cancer activity of targeted pro-apoptopic peptides." *Nature Medicine* 5(9):1032-1038.

Ellerby HM, Lee S, Andrusiak R, Ellerby LM, Chen S, Kiyota T, del Rio G, Sugihara G, Arap W, Bredesen DE & Pasqualini R (2003). An artificially designed pore-forming protein with anti-tumor effects. In press, J.B.C..

Javadpour M, Juban M, Lo W, Bishop S, Alberty J, Cowell S, Becker C, & McLaughlin M. De novo antimicrobial peptides with low mammalian cell toxicity. *J. Med. Chem.* **39**, 3107-3113 (1996).

Bibliography

Arap W, Pasqualini R, & Ruoslahti E. Cancer treatment by targeted drug delivery to tumor vasculature in a mouse model. *Science* **279**:377-380 (1998).

Arap W, Haedicke W, Bernasconi M, Kain R, Rajotte D, Krajewski S, Ellerby HM, Bredesen DE, Pasqualini R, Ruoslahti E (2002). Targeting the prostate for destruction through a vascular address. *PNAS* 99(3):1527-31.

del Rio G, Castro-Obregon S, Rao R, Ellerby HM, Bredesen DE (2001). APAP, a sequence-pattern recognition approach identifies substance P as a potential apoptotic peptide. *FEBS Lett.* 494(3):213-9.

Ellerby HM, Arap W, Ellerby LM, Kain R, Andrusiak R, Del Rio G, Krajewski S, Lombardo CR, Rao R, Ruoslahti E, Bredesen DE, Pasqualini R (1999). Anti-cancer activity of targeted pro-apoptopic peptides." *Nature Medicine* 5(9):1032-1038.

Ellerby HM, Lee S, Andrusiak R, Ellerby LM, Chen S, Kiyota T, del Rio G, Sugihara G, Arap W, Bredesen DE & Pasqualini R (2003). An artificially designed pore-forming protein with anti-tumor effects. In press *JBC*.

Javadpour M, Juban M, Lo W, Bishop S, Alberty J, Cowell S, Becker C, & McLaughlin M. De novo antimicrobial peptides with low mammalian cell toxicity. *J. Med. Chem.* **39**, 3107-3113 (1996).

List of Personnel

(5/1/02-4/30/03)
H. Michael Ellerby, Ph.D., PI
Dale E. Bredesen, M.D.
Patricia Spillman (October 2001-Present)

Appendices

1. Ellerby, H. M. et al. Anti-cancer activity of targeted pro-apoptotic peptides. *Nat Med* 5, 1032-8 (1999).

2. del Rio, G., Castro-Obregon, S., Rao, R., Ellerby, H. M. & Bredesen, D. E. APAP, a sequence-pattern recognition approach identifies substance P as a potential apoptotic peptide. *FEBS Lett* 494, 213-9. (2001).

3 Arap, W. et al. Targeting the prostate for destruction through a vascular address. *Proc Natl Acad Sci U S A* 99, 1527-1531 (2002).

4 Ellerby HM, Lee S, Andrusiak R, Ellerby LM, Chen S, Kiyota T, del Rio G, Sugihara G, Bredesen DE, Arap W, & Pasqualini R (2003). An artificially designed pore-forming protein with anti-tumor effects. *J. Biol. Chem., in press.*

Turning on tumor apoptosis

HIV-1 Nef gets macrophages moving

Genetic determinants of sleep patterns

Painful stimulation supresses joint inflammation

Insulin-specific T cells in diabetic mice

E1A induces oncogenic fusion in Ewing sarcoma

Anti-cancer activity of targeted pro-apoptotic peptides

H. Michael Ellerby, Wadih Arap, Lisa M. Ellerby, Renate Kain, Rebecca Andrusiak,
Gabriel Del Rio, Stanislaw Krajewski, Christian R. Lombardo, Rammohan Rao,
Erkki Ruoslahti, Dale E. Bredesen & Renata Pasqualini

Program on Aging and Cancer and Program on Cell Adhesion, The Burnham Institute,
10901 North Torrey Pines Rd., La Jolla, California 92037, USA
H.M.E., L.M.E., G.D.R., R.R. & D.E.B. present address: The Buck Center for Research in Aging,
8001 Redwood Blvd, Novato, California 94945, USA
R.K. present address: Clinical Institute for Clinical Pathology, Dept. Ultrastructural Pathology and Cell Biology,
University of Vienna/AKH Wien, Währinger Gürtel 18-20, A-1090 Wien, Austria
W.A. & R.P. present address: The University of Texas M.D. Anderson Cancer Center,
1515 Holcombe Boulevard, Houston, Texas 77030, USA
Correspondence should be addressed to E.R., D.B. or R.P.; emails: ruoslahti, dbredesen or pasqualini@burnham-inst.org

We have designed short peptides composed of two functional domains, one a tumor blood vessel 'homing' motif and the other a programmed cell death-inducing sequence, and synthesized them by simple peptide chemistry. The 'homing' domain was designed to guide the peptide to targeted cells and allow its internalization. The pro-apoptotic domain was designed to be non-toxic outside cells, but toxic when internalized into targeted cells by the disruption of mitochondrial membranes. Although our prototypes contain only 21 and 26 residues, they were selectively toxic to angiogenic endothelial cells and showed anti-cancer activity in mice. This approach may yield new therapeutic agents.

Tumor cell survival, growth and metastasis require persistent new blood vessel growth[1-3] (angiogenesis). Consequently, a strategy has emerged to treat cancer by inhibiting angiogenesis[4]. Peptides have been described that selectively target angiogenic endothelial cells[5-8]. Conjugates made from these peptides and the anti-cancer drug doxorubicin induce tumor regression in mice with a better efficacy and a lower toxicity than doxorubicin alone[8]. There is also a functional class of cell death-inducing receptors, or 'dependence receptors', which have embedded pro-apoptotic amino-acid sequences[9,10]. These peptide domains are required for apoptosis induction by these receptors. The peptide fragments are thought to be released into the cytosol as cleavage products of caspase proteolysis, where they induce or potentiate apoptosis through unknown mechanisms[9,10]. However, such peptides, and structurally similar pro-apoptotic antibiotic peptides, although they remain relatively non-toxic outside of eukaryotic cells, induce mitochondrial swelling and mitochondria dependent cell-free apoptosis[10,11].

There are more than 100 naturally occurring antibiotic peptides, and their de novo design has received much attention[12-14]. Many of these peptides are linear, cationic and α-helix-forming. Some are also amphipathic, with hydrophobic residues distributed on one side of the helical axis and cationic residues on the other[15]. Because their cationic amino acids are attracted to the head groups of anionic phospholipids, these peptides preferentially disrupt negatively charged membranes. Once electrostatically bound, their amphipathic helices distort the lipid matrix (with or without pore formation), resulting in the loss of membrane barrier function[15,16]. Both prokaryotic cytoplasmic membranes and eukaryotic mitochondrial membranes (both the inner and the outer) maintain large transmembrane potentials, and have a high content of anionic phospholipids, reflecting

the common ancestry of bacteria and mitochondria[15-19]. In contrast, eukaryotic plasma membranes (outer leaflet) generally have low membrane potentials, and are almost exclusively composed of zwitterionic phospholipids[16,18,20]. Many antibacterial peptides, therefore, preferentially disrupt prokaryotic membranes and eukaryotic mitochondrial membranes rather than eukaryotic plasma membranes.

If such nontoxic peptides were coupled to tumor targeting peptides that allow receptor-mediated internalization, the chimeric peptide would have the means to enter the cytosol of targeted cells, where it would be toxic by inducing mitochondrial-dependent apoptosis[10,11]. Thus, we designed targeted pro-apoptotic peptides composed of two functional domains. The targeting domain was designed to guide the 'homing' pro-apoptotic peptides to targeted cells and allow their internalization[8,21,22]. The pro-apoptotic domain was designed to be non-toxic outside of cells, but toxic when internalized into targeted cells by the disruption of mitochondrial membranes.

Design of the pro-apoptotic peptide
A computer-generated model and the sequence of one of our prototypes are shown in Fig. 1. For the targeting domain, we used either the cyclic (disulfide bond between cysteines) CNGRC peptide (Fig. 1) or the double-cyclic ACDCRGDCFC peptide (called RGD-4C), both of which have 'tumor-homing' properties[5,8] and for which there is evidence of internalization[8,21,22]. We synthesized this domain from all-L amino acids because of the presumed chiral nature of the receptor interaction. For the pro-apoptotic domain, we selected the synthetic 14-amino-acid peptide KLAKLAKKLAKLAK (Fig. 1), called (KLAKLAK)$_2$, because it killed bacteria at concentrations 1% of those required to kill eukaryotic cells[13]. We used the all-D enan-

ĆNGRĆ – GG – KLAKLAKKLAKLAK
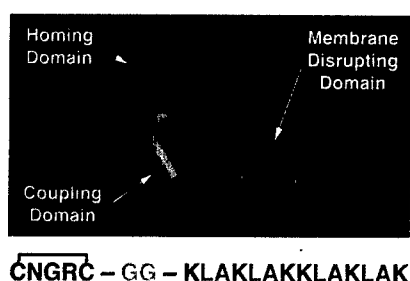
Fig. 1 Computer-generated model and amino-acid sequence of CNGRC-GG$_D$(KLAKLAK)$_2$. This peptide is composed of a 'homing' domain (blue) and a membrane-disrupting (pro-apoptotic) domain (red hydrophilic and green hydrophobic residues), joined by a coupling domain (yellow).

tiomer $_D$(KLAKLAK)$_2$ to avoid degradation by proteases[12,23]. This strategy was possible because such peptides disrupt membranes by chiral-independent mechanisms[23,24]. We coupled the targeting (CNGRC or RGD-4C) and pro-apoptotic $_D$(KLAKLAK)$_2$ domains with a glycinylglycine bridge (Fig. 1) to impart peptide flexibility and minimize potential steric interactions that would prevent binding and/or membrane disruption.

D(KLAKLAK)2 disrupts mitochondrial membranes

We evaluated the ability of $_D$(KLAKLAK)$_2$ to disrupt mitochondrial membranes preferentially rather than eukaryotic plasma membranes by mitochondrial swelling assays, in a mitochondria-dependent cell-free system of apoptosis, and by cytotoxicity assays[10]. There was morphological evidence of damage to mitochondrial membranes by electron microscopy. The peptide $_D$(KLAKLAK)$_2$ induced considerable mitochondrial swelling at a concentration of 10 μM (Fig. 2a). Mild swelling was evident even at 3 μM (data not shown), 1% the concentration required to kill eukaryotic cells (approximately 300 μM), as determined by the lethal concentration required to kill 50% of a cell monolayer (LC$_{50}$; Table 1). These results demonstrate that $_D$(KLAKLAK)$_2$ preferentially disrupts mitochondrial membranes rather than eukaryotic plasma membranes. Moreover, the peptide activated mitochondria-dependent cell-free apoptosis in a system composed of mitochondria suspended in cytosolic extract[10], as measured by characteristic caspase-3-processing from an inactive zymogen to active protease[25] (Fig. 2b). A non-α-helix-forming peptide, DLSLARLATARLAI (negative control), did not induce mitochondrial swelling (Fig. 2a), was inactive in the cell-free system (Fig. 2b) and was not lethal to eukaryotic cells[10]. We also analyzed morphologic alterations in isolated mitochondria

by electron microscopy. The peptide $_D$(KLAKLAK)$_2$ induced abnormal mitochondrial morphology, whereas the control peptide DLSLARLATARLAI did not (Fig. 2c).

Targeted pro-apoptotic peptides induce apoptosis

We evaluated the efficacy and specificity of CNGRC-GG-$_D$(KLAKLAK)$_2$ in KS1767 cells, derived from Kaposi sarcoma[26,27] (Fig. 3a–d), and MDA-MB-435 human breast carcinoma cells[5,8] (Table 1). We used KS1767 cells because they bind the CNGRC targeting peptide just as endothelial cells do. This may relate to the endothelial origin of the KS1767 cells[27]. We used MDA-MB-435 cells as negative control cells because they do not bind the CNGRC targeting peptide[8]. Although CNGRC-GG-$_D$(KLAKLAK)$_2$ was considerably toxic to KS1617 cells, an equimolar mixture of uncoupled CNGRC and $_D$(KLAKLAK)$_2$ (negative control), or $_D$(KLAKLAK)$_2$ alone, was much less toxic, indicative of a targeting effect (Table 1). In contrast, CNGRC-GG-$_D$(KLAKLAK)$_2$ was not very toxic to MDA-MB-435 cells, which do not bind the CNGRC peptide (Table 1). The other targeted peptide (RGD-4C)-GG-$_D$(KLAKLAK)$_2$, showed toxic effects similar to those of CNGRC-GG-$_D$(KLAKLAK)$_2$ on KS1617 cells, whereas an equimolar mixture of uncoupled RGD-4C and $_D$(KLAKLAK)$_2$, used as a negative control, was not very toxic (Table 1; Fig. 3c–d).

Although evidence for internalization of CNGRC and RGD-4C into the cytosol of cells has been published[5,8,21,22], we directly demonstrated internalization using biotin-labeled peptides. CNGRC–biotin, but not untargeted CARAC–biotin, was internalized into the cytosol of cells (Fig. 3e–f). We also obtained direct evidence for internalization from experiments based on cell fractionation and mass spectrometry. CNGRC-GG-$_D$(KLAKLAK)$_2$, but not CARAC-GG-$_D$(KLAKLAK)$_2$, was indeed internalized and could be detected in mitochondrial as well as cytosolic fractions (data not shown).

Next, we evaluated the efficacy and specificity of CNGRC-GG-$_D$(KLAKLAK)$_2$ in a tissue culture model of angiogenesis[28]. During angiogenesis, capillary endothelial cells proliferate and migrate[1,2]. Cord formation is a type of migration that can be studied *in vitro* by a change in endothelial cell morphology from the usual 'cobblestones' to chains or cords of cells[27]. We tested the effect of CNGRC-GG-$_D$(KLAKLAK)$_2$ on normal human dermal microvessel endothelial cells (DMECs) in the angiogenic conditions of proliferation and cord formation and in the angiostatic condition of a monolayer maintained at 100% confluency.

The treatment of DMECs with 60 μM CNGRC-GG-$_D$(KLAK-LAK)$_2$ led to a decrease in the percent viability over time compared with that of untreated controls, in the conditions of proliferation (Fig. 4a) or cord formation (Fig. 4b). In contrast, treatment with the untargeted peptide $_D$(KLAKLAK)$_2$ as a negative control led to a negligible loss in viability. Furthermore, the LC$_{50}$ for proliferating or migrating DMECs treated with CNGRC-GG-$_D$(KLAKLAK)$_2$ was 10% of the LC$_{50}$ for angiostatic DMECs maintained in a monolayer at 100% confluency (Table 1). This result indicates that CNGRC-GG-$_D$(KLAKLAK)$_2$ kills cells in angiogenic but not angiostatic conditions. The LC$_{50}$ for the untargeted control $_D$(KLAKLAK)$_2$ in angiogenic con-

Table 1 LC$_{50}$ (μM) for eukaryotic cells treated with targeted pro-apoptotic peptides

	DMEC			KS1767	MDA-MB-435
	Angiostatic	Angiogenic			
		Proliferation	Cord Form	Proliferation	Proliferation
$_D$(KLAKLAK)$_2$	492	346	368	387	333
CNGRC-GG-$_D$(KLAKLAK)$_2$	481	51[a]	34[a]	42[a]	415
(RGD-4C)-GG-$_D$(KLAKLAK)$_2$	–	–	–	10[a]	–

Results are means of three independent experiments. [a]$P<0.03$, t-test.
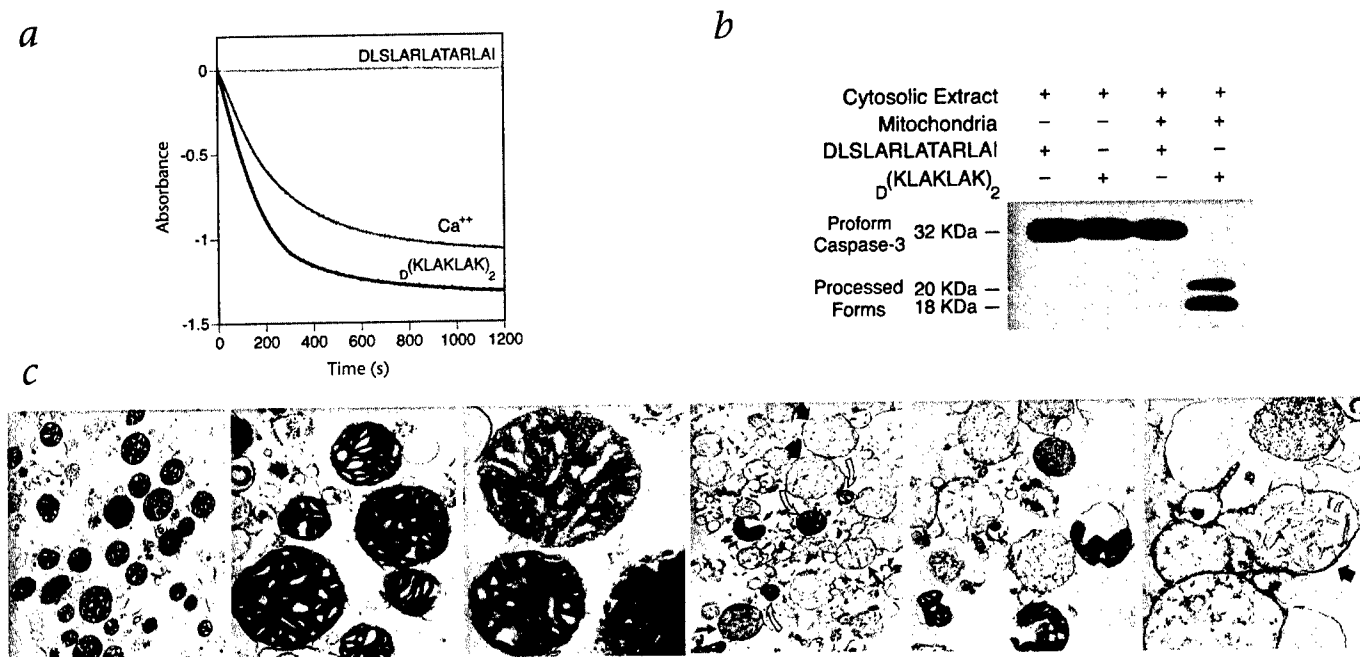
Fig. 2 $_D$(KLAKLAK)$_2$ disrupts mitochondrial membranes. **a**, $_D$(KLAKLAK)$_2$ or Ca^{2+} (positive control) induced mitochondrial swelling, whereas the non-α-helix-former DLSLARLATARLAI (negative control) did not, as shown by mitochondrial swelling curves (optical absorbance spectrum). **b**, $_D$(KLAKLAK)$_2$ activates cell-free apoptosis in a system composed of normal mitochondria and cytosolic extract, but DLSLARLATARLAI does not. An immunoblot of caspase-3 cleavage from proform (32-kDa) to processed forms (18- and 20-kDa) demonstrates a mitochondria-dependent cell-free apoptosis (left margin, sizes). Results were reproduced in two independent experiments. **c**, Morphologic alterations in isolated mito- chondria analyzed by electron microscopy. Mitochondria incubated for 15 min with 3 µM DLSLARLATARLAI show normal morphology (left panels). In contrast, mitochondria incubated for 15 min with 3 µM $_D$(KLAKLAK)$_2$ show extensive morphological changes. The damage to mitochondria progressed from the stage of focal matrix resolution (short black arrow), through homogenization and dilution of condensed matrix content with sporadic remnants of cristae (long black arrows), to extremely swollen vesicle-like structures (thick black arrows; bottom right, higher magnification); few mitochondria had normal morphology (open arrows). Ultrathin sections are shown. Original magnification, ×4,000–×40,000.

ditions was similar to the LC$_{50}$ for CNGRC-GG-$_D$(KLAKLAK)$_2$ under angiostatic conditions. An equimolar mixture of uncoupled $_D$(KLAKLAK)$_2$ and CNGRC, a non-targeted form CARAC-GG-$_D$(KLAKLAK)$_2$, and a 'scrambled' form, CGRNC-GG-$_D$(KLAK-LAK)$_2$, all gave results similar to those of $_D$(KLAKLAK)$_2$.

We also studied the mitochondrial morphology of DMECs in the condition of proliferation, after treatment with 60 µM CGRNC-GG-$_D$(KLAKLAK)$_2$ or untargeted $_D$(KLAKLAK)$_2$. The mitochondria in intact DMECs treated for 24 hours with the equimolar mixture CNGRC and $_D$(KLAKLAK)$_2$ remained morphologically normal (Fig. 4d), whereas those treated with CGRNC-GG-$_D$(KLAKLAK)$_2$ showed altered mitochondrial morphology, evident in approximately 80% of cells (Fig. 4e), before the cells rounded-up. Ultimately, the DMECs treated with CNGRC-GG-$_D$(KLAKLAK)$_2$ showed the classic morphological indicators of apoptosis, including nuclear condensation and fragmentation, as seen at 72 hours (Fig. 4 f and g)(ref. 10). Apoptotic cell death (Fig. 4g) was confirmed with an assay for
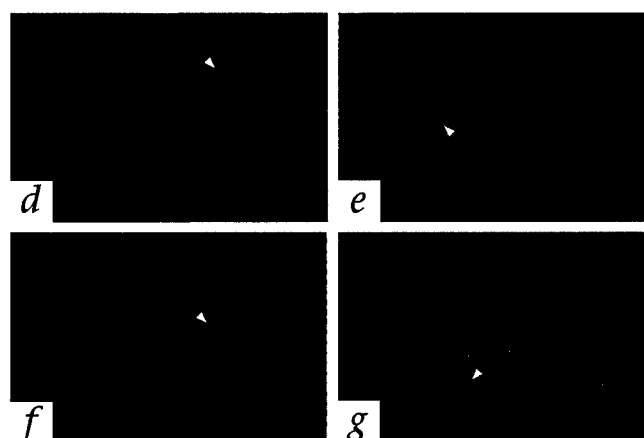

Fig. 3 CNGRC-GG-$_D$(KLAKLAK)$_2$ and (RGD-4C)-GG-$_D$(KLAKLAK)$_2$ induce apoptosis. **a**, KS1767 cells treated with 100 µM of non-targeted CARAC-GG-$_D$(KLAK-LAK)$_2$ (negative control) remain unaffected after 48 h. **b**, KS1767 cells treated with 100 µM of CNGRC-GG-$_D$(KLAKLAK)$_2$ undergo apoptosis, as shown at 48 h. Condensed nuclei and plasma membrane blebbing are evident. **c**, KS1767 cells treated with 10 µM of an equimolar mixture of (RGD-4C) and $_D$(KLAKLAK)$_2$ (negative control) remain unaffected after 48 h. **d**, KS1767 cells treated with 10 µM of (RGD-4C)-GG-$_D$(KLAKLAK)$_2$ undergo apoptosis, as shown at 48 h. Condensed nuclei and plasma membrane blebbing are evident. Scale bar represents 250 µm. **e** and **f**, KS1767 cells treated with 100 µM of CNGRC-biotin (**e**) or CARAC-biotin (**f**) for 24 h and subsequently treated with streptavidin FITC demonstrate internalization of CNGRC-biotin, but not CARAC-biotin, into the cytosol.
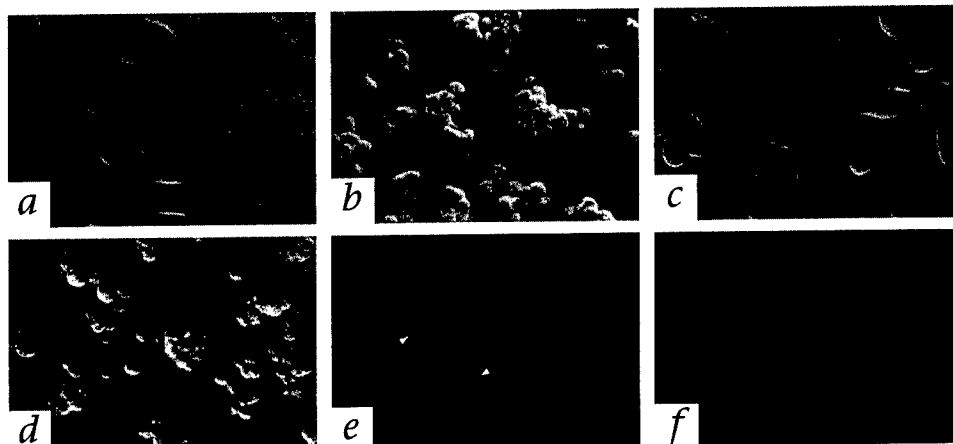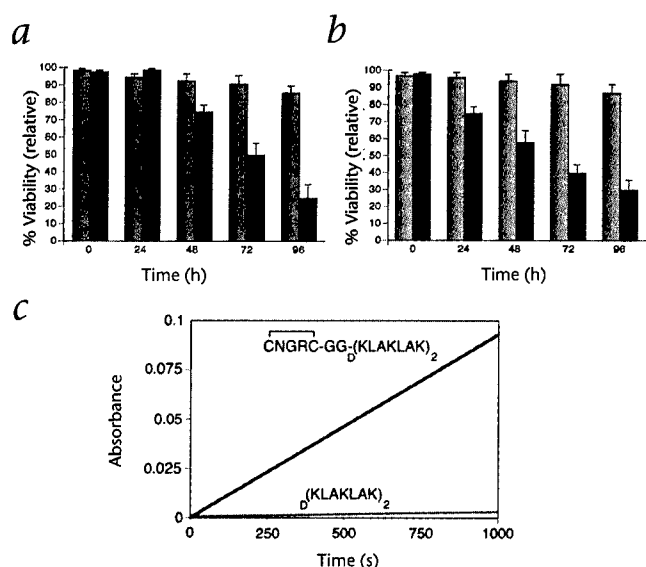
Fig. 4 CNGRC-GG-$_D$(KLAKLAK)$_2$ induces apoptosis and mitochondrial swelling in DMECs. **a**, Proliferating DMECs treated with CNGRC-GG-$_D$(KLAKLAK)$_2$ (filled bars) lose viability (apoptosis) over time ($P<$ 0.02), but those treated with the control peptide $_D$(KLAKLAK)$_2$ (gray bars) do not ($P<$ 0.05). **b**, Cord-forming DMECs lose viability (apoptosis) over time (filled bars), but those treated with $_D$(KLAKLAK)$_2$ (gray bars) do not ($P<$ 0.05). **c**, Apoptotic cell death was confirmed with an assay for caspase 3 activity, as shown by the hydrolysis of DEVD-pNA with time. Results were reproduced in three independent experiments. **d**, Proliferating DMECs show normal nu-

clear (blue) and mitochondrial (red) morphology after 24 h of treatment with a mixture of 100 μM $_D$(KLAKLAK)$_2$ and CNGRC. **e–g**, Proliferating DMECs treated with 100 μM CNGRC-GG-$_D$(KLAKLAK)$_2$. After 24 h (**e**), cells show normal nuclear (blue) but abnormal mitochondrial (red) morphology. Mitochondrial swelling and dysfunction is shown by a decrease in fluorescence intensity and a change in morphology from an extended lace-like network to a condensed clumping of spherical structures. Classic morphological indicators of mid- to late apoptosis (for example, condensed and fragmented nuclei) are evident at 48 h (**f**) and 72 h (**g**) (arrow).

---

caspase 3 activity[10]. We also tested a caspase inhibitor for its effect on cell death induced by CNGRC-GG-$_D$(KLAKLAK)$_2$. We used Kaposi sarcoma cells, as these cells bind CNGRC. The inhibitor zVAD.fmk, at a concentration (25 μM) that inhibits caspases but not non-caspase proteases, inhibited the cell death induced by CNGRC-GG-$_D$(KLAKLAK)$_2$ (data not shown). This result is compatible with the earlier demonstration that the

CNGRC-GG-$_D$(KLAKLAK)$_2$ peptide is pro-apoptotic. Although the relatively early mitochondrial swelling is consistent with the putative mechanism of action, that is, a direct activation of the apoptotic machinery, we cannot rule out the possibility that the peptides actually kill by inducing some irreversible damage to cells which then activates the apoptotic program.

In addition to the fluorescence studies shown above, we studied cultured cells by electron microscopy to confirm that CNGRC-GG-$_D$(KLAKLAK)$_2$ induces abnormal mitochondrial morphology in intact cells (Fig. 5). Kaposi sarcoma-derived KS1767 cells treated with the control peptide CARAC-GG-$_D$(KLAKLAK)$_2$ for 72 hours showed no overall changes, with no or very minor changes in the mitochondria (Figs. 5a–c). In contrast, the mitochondria in KS1767 cells incubated for 12 hours
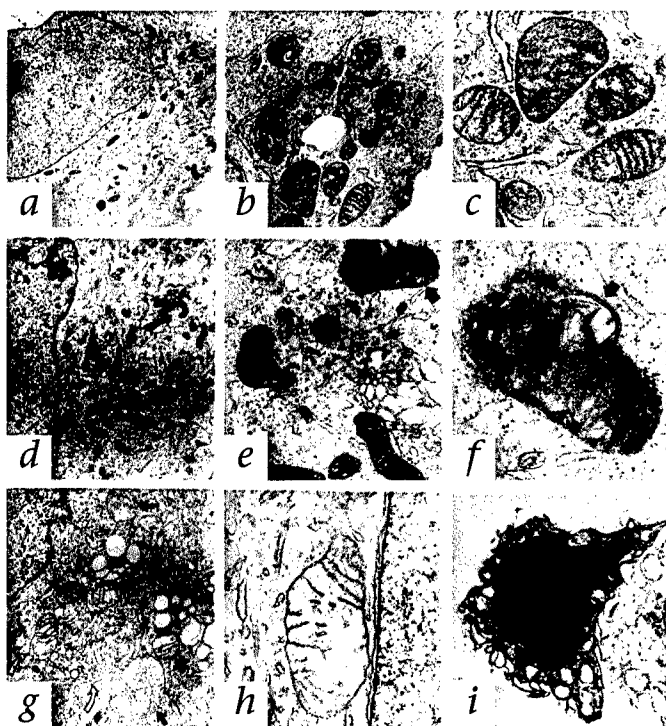
Fig. 5 Electron microscopic studies of cultured cells. a–c, KS1767 cells treated with 100 μM CARAC-GG-$_D$(KLAKLAK)$_2$ for 72 h show the representative ultrastructural details of normal cells, with no or negligible changes seen in the mitochondria. Original magnifications: **a**, ×4,000; **b**, ×25,000; **c**, ×45,000. **d–f**, In contrast, the mitochondria in KS1767 cells incubated for 12 h with 100 μM CNGRC-GG-$_D$(KLAKLAK)$_2$ begin to show a condensed appearance and vacuolization despite a relatively normal cell morphology (black arrows). Original magnifications: **d**, ×12,000; **e**, ×20,000; **f**, ×45,000). **g** and **h**, Progressive damage to KS1767 cells is evident after 24 h, when many mitochondria show typical large matrix compartments and prominent cristae, ultrastructural features of low level of oxidative phosphorylation. Original magnifications: **g**, ×12,000; **h**, ×40,000. Some of the swollen mitochondria (**g**, black arrows) are similar in appearance to those in isolated mitochondria treated with 100 μM $_D$(KLAKLAK)$_2$ (Fig. 2c, bottom right). **i**, In some cells, this process progressed to a final stage, with extensive vacuolization and the pyknotic, condensed nuclei typical of apoptosis. Original magnification, ×8,000.
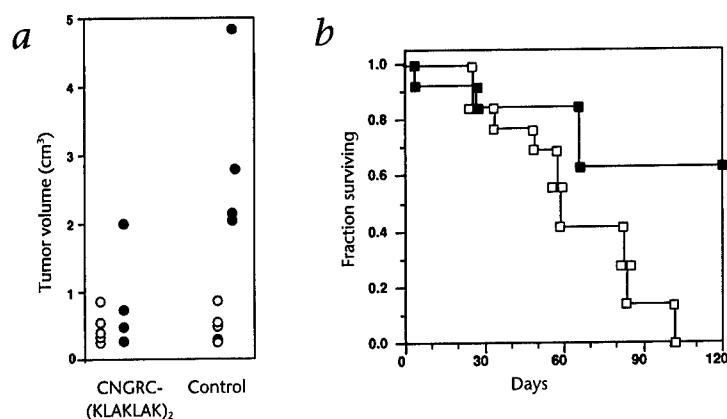
Fig. 6 Treatment of nude mice bearing MDA-MB-435-derived human breast carcinoma xenografts with CNGRC-GG-$_D$(KLAKLAK)$_2$. **a**, Tumors treated with CNGRC-GG-$_D$(KLAKLAK)$_2$ are smaller than control tumors treated with CARAC-GG-$_D$(KLAKLAK)$_2$, as shown by differences in tumor volumes between day 1 (O) and day 50 (●). $P = 0.027$, t-test. One mouse in the control group died before the end of the experiment. **b**, Mice treated with CNGRC-GG- $_D$(KLAKLAK)$_2$ (■) survived longer than control mice treated with an equimolar mixture of $_D$(KLAKLAK)$_2$ and CNGRC (□), as shown by a Kaplan-Meier survival plot ($n = 13$ animals/group). $P < 0.05$, log-rank test.

Treatment of nude mice bearing human tumor xenografts with CNGRC-GG-$_D$(KLAKLAK)$_2$ and (RGD-4C)-GG-$_D$(KLAKLAK)$_2$

Given our results in culture, we proceeded to test both targeted pro-apoptotic peptides *in vivo*, using nude mice with human MDA-MD-435 breast carcinoma xenografts. Tumor volume in the groups treated with CNGRC-GG-$_D$(KLAKLAK)$_2$ was on average 10% that of control groups (Fig. 6*a*); survival was also longer in these groups than in control groups (Fig. 6*b*). The control was a non-targeted 'mimic' CARAC-GG-$_D$(KLAKLAK)$_2$ peptide; the CARAC sequence has a charge, size and general structure similar to that of CNGRC. Some of the mice treated with CNGRC-GG-$_D$(KLAKLAK)$_2$ outlived control mice by several months, indicating that both primary tumor growth and metastasis were inhibited by CNGRC-GG-$_D$(KLAKLAK)$_2$. Treatment in nude mice bearing MDA-MD-435 breast carcinoma xenografts with (RGD-4C)-GG-$_D$(KLAKLAK)$_2$ also resulted in a significantly reduced tumor and metastatic burden (Fig. 7). Experimental parameters included tumor volumes before and after treatment (Fig. 7*a*), wet weights of the tumors (Fig. 7*b*, right) and weight of lung metastases (Fig. 7*b*, left). The control group was treated with an equimolar mixture of RGD-4C and $_D$(KLAKLAK)$_2$. Histopathological and TUNEL analysis showed cell death in the treated tumors and evidence of apoptosis and necrosis (data not shown).

To assess toxicity in mice without tumors, we have administered CNGRC-GG-$_D$(KLAKLAK)$_2$ or (RGD-4C)-GG-$_D$(KLAKLAK)$_2$ to both immunocompetent (balb/c) and to immunodeficient (balb/c nude) mice at a dose of 250 μg/mouse per week for eight doses. No apparent toxicities have been found in 3 months. Moreover, in these conditions, the peptides are not immunogenic, as determined by ELISA of blood obtained from the immunocompetent mice (data not shown).

We have also evaluated the stability of the CNGRC-GG-$_D$(KLAKLAK)$_2$ and (RGD-4C)-GG-$_D$(KLAKLAK)$_2$ peptides *ex vivo* and in mice. We analyzed the two targeted peptides using mass spectrometry. In the first set of experiments, the targeted peptides were pre-mixed with whole blood and incubated at 37 °C.

with CNGRC-GG-$_D$(KLAKLAK)$_2$ showed abnormal condensation and vacuolization despite a relatively preserved cell morphology (Fig. 5*d–f*, black arrows). Progressive cellular damage could be seen after 24 hours, when many mitochondria showed ultrastructural features of low-level oxidative phosphorylation (Fig. 5*g* and *h*); in later stages, some of the damaged mitochondria (Fig. 5g, black arrows) showed profound changes, as seen in the isolated mitochondria treated with $_D$(KLAKLAK)$_2$ (Fig. 2*c*, right lower panel). In some cells, this process progressed to a late apoptotic stage. Typical vacuolization and condensed nuclei became evident (Fig. 5*i*). These results show that the mitochondria underwent changes in morphology and function that were well-represented by a progression from a state of normal morphology and normal oxidative phosphorylation (Fig. 5*a*) to a state of condensed morphology and a high rate of oxidative phosphorylation (Fig. 5*d*) to a final edemic state (Fig. 5*g*) associated with a low energy level.
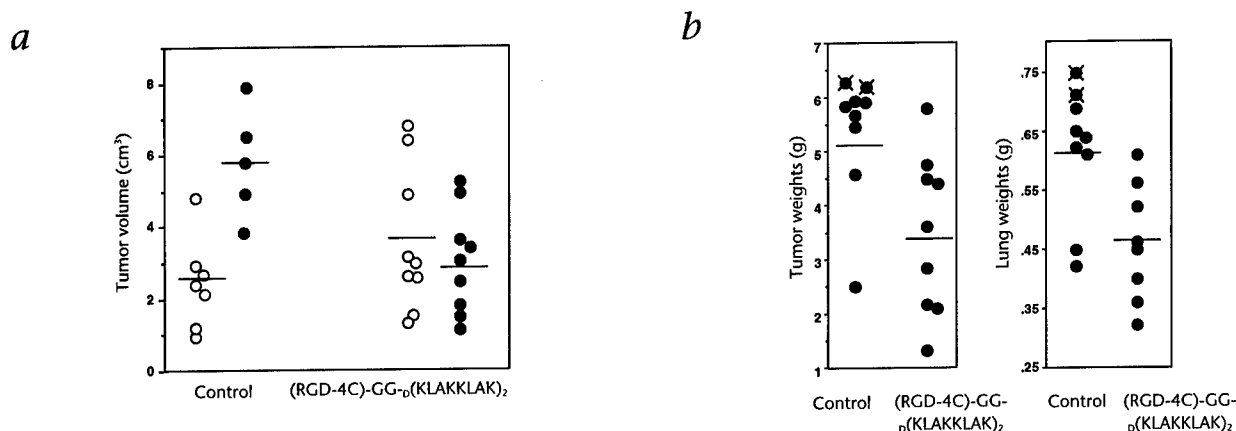

Fig. 7 Treatment of nude mice bearing MDA-MB-435-derived human breast carcinoma xenografts with (RGD-4C)-GG-$_D$(KLAKLAK)$_2$. **a**, Tumors treated with (RGD-4C)-GG-$_D$(KLAKLAK)$_2$ are smaller than control tumors treated with an equimolar mixture of RGD-4C peptide and $_D$(KLAKLAK)$_2$. Tumor volumes were assessed on day 1 (O) and day 90 (●). $P = 0.027$, t-test. **b**, Tumor weights (right) and lung metastatic burden (left) are also decreased in mice treated with (RGD-4C)-GG-$_D$(KLAKLAK)$_2$; these were measured when the experiment ended, on day 110 ($n = 9$ animals/group). $P < 0.05$, t-test.

The peptides were intact up to 1 hour in these conditions. In the second set of experiments, mice were injected intravenously with the two targeted peptides and blood samples were analyzed; the peptides were present at 10 minutes after administration (data not shown). We chose these short circulation times to coincide with the experimental conditions established for 'homing' of targeted peptides *in vivo*[5,7,8].

Targeted pro-apoptotic peptides represent a potential new class of anti-cancer agents; their activity may be optimized for maximum therapeutic effect by adjusting properties such as residue placement, domain length, peptide hydrophobicity and hydrophobic moment[29]. Beyond this, future targeted pro-apoptotic peptides might be designed to disrupt membranes using a completely different type of pro-apoptotic domain such as β-strand/sheet-forming peptides[30]. Our results provide a glimpse at a new cancer therapy combining two levels of specificity: 'homing' to targeted cells and selective apoptosis of such cells after entry.

Methods

Reagents. Human recombinant vascular endothelial growth factor (VEGF; PharMingen, San Diego, California), antibody against caspase-3 (Santa Cruz Biotechnology, Santa Cruz, California), streptavidin FITC (Sigma) and N-acetyl-Asp-Glu-Val-Asp-pNA (DEVD-pNA; BioMol, Plymouth Meeting, Pennsylvania) were obtained commercially. Peptides were synthesized to our specifications at greater than 90% purity by HPLC (DLSLARLATARLAI, Coast (San Diego, California); all other peptides, AnaSpec (San Jose, California).

The computer-generated model was made with Insight II (Molecular Simulations, San Diego, California) running on an O_2 work station (Silicon Graphics, Mountain View, California)

Cell culture. Dermal microvessel endothelial cells (DMECs) were grown in CADMEC Growth Media™ (media and cells from Cell Applications, San Diego, California). DMECs were then cultured in three experimental conditions: proliferation (30% confluency in a growth media supplemented with 500 ng/ml VEGF); no proliferation (100% confluency in media formulated to maintain a monolayer); and cord formation (60% confluency (required for induction) in media formulated to induce cord formation). KS1767 and MDA-MB-435 cells were cultured as described[5,8,27,28].

Internalization assay. KS1767 cells grown on coverslips were treated with 100 μM biotin-labeled CNGRC or biotin-labeled CARAC (negative control) for 24 h. Streptavidin FITC was added to the coverslips, and cells were then viewed on an inverted microscope (Nikon TE 300) using a FITC filter.

Mitochondrial swelling assays. Rat liver mitochondria were prepared as described[10]. The concentrations used were 10 μM $_D$(KLAKLAK)$_2$, 10 μM DL-SLARLATARLAI (negative control), or 200 μM Ca^{2+} (positive control). The peptides were added to mitochondria in a cuvette, and swelling was quantified by measuring the optical absorbance at 540 nm.

Cell-free apoptosis assays. Cell-free systems were reconstituted as described[10]. For the mitochondria-dependent reactions, rat liver mitochondria were suspended in normal (non-apoptotic) cytosolic extracts of DMECs. The peptides were added at a concentration of 100 μM. After incubation for 2 h at 30 °C or 37 °C, mitochondria were removed by centrifugation, and the supernatant was analyzed by SDS–PAGE and immunoblotting (12% gels, BioRad, Richmond, California). Proteins were transferred to PVDF membranes (BioRad, Richmond, California) and incubated with antibody against caspase-3, followed by ECL detection (Amersham).

Caspase activity of cell lysates. The caspase activity of DMEC lysates was measured as described[10]. Aliquots of cell lysates (1 μl lysate; 8–15 mg/ml) were added to 100 μM DEVD-pNA (100 μl; 100 mM HEPES, 10% sucrose, 0.1% CHAPS and 1 mM DTT, pH 7.0). Hydrolysis of DEVD-pNA was monitored by spectrophotometry (400 nm) at 25 °C.

Morphological quantification of cellular apoptosis. Percent viability and LC_{50} (Table 1) were determined by apoptotic morphology[10]. For the percent viability assay, DMECs were incubated with 60 μM active peptide or control peptide. Cell culture medium was aspirated at various times from adherent cells, and the cells were gently washed once with PBS at 37 °C. Then, a 20-fold dilution of the dye mixture (100 μg/ml acridine orange and 100 μg/ml ethidium bromide) in PBS was gently pipetted on the cells, which were viewed on an inverted microscope (Nikon TE 300). The cell death seen was apoptotic cell death and was confirmed by a caspase activation assay. Not all cells progressed through the stages of apoptosis at the same time. At the initial stages, a fraction of the cells were undergoing early apoptosis. At later stages, this initial fraction had progressed to late apoptosis and even to the necrotic-like stage associated with very late apoptosis (for example, loss of membrane integrity in apoptotic bodies). However, these cells were joined by a new fraction undergoing early apoptosis. Thus, cells with nuclei showing margination and condensation of the chromatin and/or nuclear fragmentation (early/mid-apoptosis; acridine orange-positive) or with compromised plasma membranes (late apoptosis; ethidium bromide-positive) were considered not viable. At least 500 cells per time point were assessed in each experiment. Percent viability was calculated relative to untreated controls. LC_{50} for monolayer, proliferation (60% confluency), and cord formation were assessed at 72 h.

Mitochondrial morphology. DMECs after 24 and 72 h of treatment with peptide were incubated for 30 min at 37 °C with a mitochondrial stain (100 nM MitoTracker Red™ CM-H$_2$XRos; the nonfluorescent, reduced form of the compound) and a nuclear stain (500 nm DAPI; Molecular Probes, Eugene, Oregon). Mitochondria were then visualized under fluorescence microscopy (100x objective) under an inverted microscope using a triple wavelength filter set (Nikon).

Electron microscopy. Rat liver mitochondria were prepared as described[10]. The mitochondria were incubated either with a control peptide (DLSLAR-LATARLAI) or with 3 μM $_D$(KLAKLAK)$_2$. The effects of the treatment were assessed at different times (Fig. 2c). Kaposi sarcoma cells were collected from 24-well Biocoat Cell culture inserts for electron microscopy (Becton Dickinson, Franklin Lakes, New Jersey). Cell monolayers at 80% confluency were exposed to either 100 μM CARAC-GG-$_D$(KLAKLAK)$_2$ (control) or CNGRC-GG-$_D$(KLAKLAK)$_2$ (targeted) (Fig. 5). All specimens were fixed with 3% glutaraldehyde in 0.1 M potassium phosphate buffer, pH 7.4 for 30 to 45 min at the room temperature, followed by postfixation with aqueous 1% osmium tetroxide and 2% uranyl acetate. After dehydration using a graded series of ethanol rinses, tissues were embedded in resin. Ultrathin sections after additional counterstainings were viewed and photographed on an electron microscope (Hitachi H-600).

Human tumor xenografts. MDA-MB-435-derived tumor xenografts were established in female nude mice 2 months old (Jackson Labs, Bar Harbor, Maine) as described[33]. The mice were anesthetized with Avertin as described[31]. The peptides were administered at a dose of 250 μg/week per mouse, given slowly through the tail vein in a volume of 200 μl. Three-dimensional measurements of tumors were made by caliper on anesthetized mice, and were used to calculate tumor volume[5,8]. Then, tumors and lungs were surgically removed and the wet weights recorded. Animal experimentation was reviewed and approved by the Institute's Animal Research Committee.

1. Risau, W. Mechanisms of angiogenesis. *Nature* **386**, 671–674 (1997).
2. Zetter, B.R. Angiogenesis and tumor metastasis. *Annu. Rev. Med.* **49**, 407–424

ARTICLES

(1998).

3. Bicknell, R. in *Tumour Angiogenesis.* (eds. Bicknell, R., Lewis, C.E. & Ferrara, N.) 19–28 (Oxford University Press, Oxford 1997).

4. Folkman, J. in *Cancer: Principles and Practice of Oncology.* (eds. DeVita, V.T., Hellman, S. & Rosenberg, S.A.) 3075–3087 (Lippincott-Raven, New York, 1997).

5. Pasqualini, R., Koivunen, E. & Ruoslahti, E. αv integrins as receptors for tumor targeting by circulating ligands. *Nature Biotechnol.* **15**, 542–546 (1997).

6. Arap, W., Pasqualini, R. & Ruoslahti, E. Chemotherapy targeted to tumor vasculature. *Curr. Opin. Oncol.* **10**, 560–565 (1998).

7. Pasqualini, R., Arap, W., Rajotte, D. & Ruoslahti, E. in *Phage Display of Proteins and Peptides* (eds. Barbas, C., Burton, D., Silverman, G. & Scott, J.) (Cold Spring Harbor, New York, in the press).

8. Arap, W., Pasqualini, R. & Ruoslahti, E. Cancer treatment by targeted drug delivery to tumor vasculature in a mouse model. *Science* **279**, 377–380 (1998).

9. Bredesen D.E. *et al.* P75(NTR) and the concept of cellular dependence – seeing how the other half die. *Cell Death Differ.* **5**, 365–371 (1998).

10. Ellerby, H.M. *et al.* Establishment of a cell-free system of neuronal apoptosis: comparison of premitochondrial, mitochondrial, and postmitochondrial phases. *J. Neurosci.* **17**, 6165–6178 (1997).

11. Mehlen, P. *et al.* The DCC gene product induces apoptosis by a mechanism requiring receptor proteolysis. *Nature* **395**, 801–804 (1998).

12. Bessalle, R., Kapitkovsky, A., Gorea, A., Shalit, I. & Fridkin, M. All-D-magainin: chirality, antimicrobial activity and proteolytic resistance. *FEBS Lett.* **274**, 151–155 (1990).

13. Javadpour, M.M. *et al. De novo* antimicrobial peptides with low mammalian cell toxicity. *J. Med. Chem.* **39**, 3107–3113 (1996).

14. Blondelle, S.E. & Houghten, R.A. Design of model amphipathic peptides having potent antimicrobial activities. *Biochemistry* **31**, 12688–12694 (1992).

15. Epand, R.M. in *The Amphipathic Helix* (CRC, Boca Raton, Florida, 1993).

16. de Kroon, A., Dolis, D., Mayer, A., Lill, R. & de Kruijff, B. Phospholipid composition of highly purified mitochondrial outer membranes of rat liver and Neurospora crassa. Is cardiolipin present in the mitochondrial outer membrane? *Biochim. Biophys. Acta* **1325**, 108–116 (1997).

17. Matsuzaki, K., Murase, O., Fujii, N. & Miyajima, K. Translocation of a channel-forming antimicrobial peptide, magainin 2, across lipid bilayers by forming a pore. *Biochemistry* **34**, 6521–6526 (1995).

18. Hovius, R., Thijssen, J., van der Linden, P., Nicolay, K. & de Kruijff, B. Phospholipid asymmetry of the outer membrane of rat liver mitochondria: Evidence for the presence of cardiolipin on the outside of the outer membrane. *FEBS Lett.* **330**, 71–76 (1993).

19. Baltcheffsky, H., & Baltcheffsky, M. in *Mitochondria and Microsomes* (eds. Lee, C.P., Schatz, G., Dallner, G.) 519–540 (Addison-Wesley, Reading, Massachusetts, 1981).

20. Daum, G. Lipids of Mitochondria. *Biochim. Biophys. Acta* **882**, 1–42 (1985).

21. Hart, S.L. *et al.* Cell binding and internalization by filamentous phage displaying a cyclic Arg-Gly-Asp-containing peptide. *J. Biol. Chem.* **269**, 12468–12474 (1994).

22. Bretscher, M.S. Endocytosis and recycling of the fibronectin receptor in CHO cells. *EMBO J.* **8**, 1341–1348 (1989).

23. Dathe, M. *et al.* Hydrophobicity, hydrophobic moment, and angle subtended by charged residues modulate antibacterial and haemolytic activity of amphipathic helical peptides. *FEBS Lett.* **403**, 208–212 (1997).

24. Alvarez-Bravo, J., Kurata, S. & Natori, S. Novel synthetic antimicrobial peptides effective against methicillin-resistant *Staphylococcus aureus. Biochem. J.* **302**, 535–538 (1994).

25. Alnemri, E.S. *et al.* ICE/CED-3 protease nomenclature. *Cell* **87**, 171 (1996).

26. Hernier, B.G. *et al.* Characterization of a human Kaposi's sarcoma cell line that induces angiogenic tumors in animals. *AIDS* **8**, 575–581 (1994).

27. Samaniego, F. *et al.* Vascular endothelial growth factor and basic fibroblast growth factor present in Kaposi's sarcoma (KS) are induced by inflammatory cytokines and synergize to promote vascular permeability and KS lesion development. *Amer. J. Path.* **152**, 1433–1443 (1998).

28. Goto, F., Goto, K., Weindel, K. & Folkman, J. Synergistic effects of vascular endothelial growth factor and basic fibroblast growth factor on the proliferation and cord formation of bovine capillary endothelial cells within collagen gels. *Lab. Invest.* **69**, 508–517 (1993).

29. Wade, D. *et al.* All-D amino acid-containing channel-forming antibiotic peptides. *Proc. Natl Acad. Sci. USA* **87**, 4761–4765 (1990).

30. Mancheno, J.M., Martinez del Pozo, A., Albar, J.P., Onaderra, M. & Gavilanes, J.G. A peptide of nine amino acid residues from α-sarcin cytotoxin is a membrane-perturbing structure. *J. Peptide Res.* **51**, 142–148 (1998).

31. Pasqualini, R. & Ruoslahti, E. Organ targeting *in vivo* using phage display peptide libraries. *Nature* **380**, 36–366 (1996).

APAP, a sequence-pattern recognition approach identifies substance P as a potential apoptotic peptide

Gabriel del Rio, Susana Castro-Obregon, Rammohan Rao, H. Michael Ellerby[1],
Dale E. Bredesen*

Buck Institute for Age Research, 8001 Redwood Blvd., Novato, CA 94945-1400, USA

Abstract We have previously described a novel cancer chemotherapeutic approach based on the induction of apoptosis in targeted cells by homing pro-apoptotic peptides. In order to improve this approach we developed a computational method (approach for detecting potential apoptotic peptides, APAP) to detect short PAPs, based on the prediction of the helical content of peptides, the hydrophobic moment, and the isoelectric point. PAPs are toxic against bacteria and mitochondria, but not against mammalian cells when applied extracellularly. Among other peptides, substance P was identified as a PAP and subsequently demonstrated to be a pro-apoptotic peptide experimentally. APAP thus provides a method to detect and ultimately improve pro-apoptotic peptides for chemotherapy. © 2001 Published by Elsevier Science B.V. on behalf of the Federation of European Biochemical Societies.

Key words: Apoptosis; Antibacterial peptide; Bioinformatics

1. Introduction

We have previously described the finding that an antibacterial peptide, when targeted intracellularly to the angiogenic vasculature (i.e. to the endothelial cells) supplying tumors, can induce apoptosis by swelling their mitochondria [1], leading to the loss of tumor blood supply and consequent tumor regression. We named these chemotherapeutic peptides homing pro-apoptotic peptides. We designed the pro-apoptotic part of the peptides to induce endothelial cell apoptosis through mitochondrial swelling. The peptides are positively charged and the mitochondria, like bacteria, have negatively charged membranes, thus the peptides are attracted to and disrupt the mitochondrial membrane [2,3]. The initial results were obtained with a 21-residue peptide, of which the carboxy-terminal 14 amino acids represented the pro-apoptotic peptide, with the amino-terminal seven amino acids comprising the targeting peptide and a glycinylglycine bridge. The therapeutic index (TI) of the initial pro-apoptotic peptides is approximately 10. In order to increase the TI and minimize

*Corresponding author. Fax: (1)-415-209 2230.
E-mail: dbredesen@buckinstitute.org

[1] Also corresponding author. E-mail: mellerby@buckinstitute.org.

Abbreviations: APAP, approach for detecting PAPs; PAPs, potential apoptotic peptides; SP, substance P; IP, isoelectric point; M, average helical hydrophobic moment; TI, therapeutic index

the length of these peptides, we designed a computational approach to detect short, linear and specific pro-apoptotic peptides.

Apoptosis in mammals and other eukaryotic organisms is a characteristic process of cell death, which can, among its other effects, limit the spread of viruses and other intracellular organisms [4]. For example, the difference in viral titer during baculoviral infection with and without apoptosis inhibition is 200–15 000-fold [4]. Thus apoptosis is a mechanism of defense against pathogenic infections.

Apoptosis proceeds by the activation of a group of cysteine proteases called caspases [5]. One of these, caspase-9, is activated when cytochrome c is released from mitochondria, which may occur with the disruption of the mitochondrial outer membrane [6]. This cytochrome c release in apoptotic cells may be induced by pro-apoptotic members of the Bcl-2 family, such as Bax and Bid, although the mechanism by which this is achieved is incompletely understood [7]. Nonetheless, the similarities between bacterial and mitochondrial membranes (and membrane potentials) suggested the possibility that there may be similarities between the effect of the antibacterial/pro-apoptotic peptides and pro-apoptotic Bcl-2 family members.

Antibacterial peptides in multicellular organisms are thought to serve as a defense against microbial pathogens. Originally found in invertebrates, antibacterial peptides have now been described in humans and many other organisms [2]. Among these peptides, the most well characterized are the short linear peptides (less than 40 amino acids in length) that do not contain cysteine residues. A characteristic shared by virtually all of these peptides is the presence of an amphipathic α-helical structure, which stabilizes in environments of hydrophobic nature [8] (although this helical structure has been shown not to be necessary for membrane lysis produced by a truncated form of pardaxin, an antibacterial peptide from the sole *Pardachirus marmoratus* [9]). Another characteristic shared by some of these peptides is selectivity, in that membranes from bacteria are targeted by these peptides more efficiently than mammalian plasma membranes. This selectivity is based on the complementary charge between the peptides, which are characteristically positively charged, and the negatively charged membranes of bacteria [2,3].

Structurally, these peptides typically adopt an unfolded conformation in aqueous solution. On contact with a membrane with a complementary charge, these peptides anchor to the membrane and assume an α-helical conformation. In that conformation, these peptides would either lie over the mem-

brane surface in a carpet-like arrangement (in which the peptide backbone lies parallel to the membrane), or penetrate it according to the barrel–stave mechanism (in which the peptide backbone lies perpendicular to the membrane) [2]. In either case, the integrity of the membrane would be disturbed, eventually leading to membrane lysis.

In order to optimize the homing pro-apoptotic peptide approach to cancer chemotherapy by maximizing the TI (see Section 2), we have developed a theoretical approach intended to model the properties of the antibacterial peptides that present selectivity for bacteria (and thus have very low toxic effects on mammalian cells when applied extracellularly). It is our goal in this work to develop a sequence-pattern recognition approach to detect peptides that will be toxic towards mitochondria but not to mammalian cells when applied extracellularly. We refer to the peptides identified by this approach as potential apoptotic peptides (PAPs), since they may induce apoptosis by swelling mitochondria when targeted intracellularly, as previously described [1]. We refer to the approach as APAP, as an abbreviation for approach for detecting PAPs. Using APAP, we searched the SwissProt database for PAPs and among other peptides we found that substance P (SP), an extensively studied neuropeptide present in mammals, birds and fish, has all the sequence characteristics of the PAPs. Furthermore, we found that SP is capable of swelling mitochondria and inducing the cleavage of caspase-3 zymogen, a known substrate of the active form of caspase-9 in vitro. As expected, SP demonstrated very low toxicity for eukaryotic cells when applied extracellularly, in addition to displaying toxicity towards bacterial cells. These results support our sequence-pattern recognition approach to identifying new PAPs, and suggest a new role for SP in the brain.

2. Materials and methods

2.1. Sequence-pattern recognition approach

We noticed that the known antibiotic peptides fit a pattern, which includes a low likelihood of helicity in aqueous solution, a high likelihood of helicity in the presence of negatively charged membranes, and a high isoelectric point (IP). We therefore calculated the helical probability of monomeric peptides in aqueous solution (AGADIR score), the IP and the hydrophobic moment to account for the characteristics of antibacterial peptides with low toxic activity against mammalian cells. We hypothesized that these characteristics are important in determining the selectivity observed in these peptides towards bacterial membranes and bacterial-like membranes (i.e. mitochondrial membranes).

A subset of 30 antibacterial peptides previously reported in the literature was used for calculations of AGADIR scores (A) [10], IP, and average helical hydrophobic moments (M) [11], (Tables 2A and 2B). The peptide sequences of this subset are shown in Table 1.

The TI of a peptide is here defined as the ratio between the inhibitory concentration observed with mammalian cells and the inhibitory concentration observed with bacterial cells (Tables 2A and 2B). The higher the value of this ratio is, the more specific the peptide is for prokaryotic (negatively charged) membranes.

PAPs were searched for in the SwissProt database, release 38 [12], which contains a total of 80 000 protein sequences. First, all of the peptide sequences of 40 or fewer amino acids in length were extracted from this database. Then all of these sequences (2473 database entries) were used to calculate their corresponding M, IP and AGADIR scores. Protein fragments, as opposed to peptides, were not considered in this study.

2.2. Computational resources

The PEPPLOT and ISOELECTRIC programs from the GCG package (Wisconsin package version 10, USA) were used to calculate M and IP, respectively. We averaged the non-zero α-values calculated by the PEPPLOT program (see Section 2) for windows of eight residues. To calculate the AGADIR score, we used the AGADIR program, which was kindly provided by Dr. Luis Serrano at EMBL. The hydrophobicity of peptide sequences was obtained by calculating the average hydrophobicity of the sequence using the consensus scale reported by Eisenberg [11]. All these programs were run on a SGI Origin 2000 server.

2.3. Caspase-3 activation in a cell-free apoptosis system induced by SP

2.3.1. Preparation of cytoplasmic extracts. Cytoplasmic extracts were prepared as described before [18]. Briefly, non-apoptotic neuronal cells were sonicated and centrifuged at $16\,000 \times g$. This extract was made free of nuclei, mitochondria and did not self-prime.

2.3.2. Preparation of mitochondria. Rat and mouse liver mitochondria were prepared as described by Hovius et al., [13], with modifications as described previously [14]. Cultured cell mitochondria were prepared as described previously [15].

2.4. Protein electrophoresis and Western blots

Electrophoresis of proteins was carried out using either 8 or 12% SDS–polyacrylamide gels. Equal amounts of total protein were loaded per lane, and the proteins were separated at 4°C at 50 V through the stacking gel, and 90 V through the separating gel.

Western blot transfer of the proteins separated by electrophoresis was carried out at 4°C using PVDF membranes (0.2 mm) (Bio-Rad), at either 200 mA for 2 h. Blots were then blocked for 1 h in TBST (10 mM Tris–HCl, pH 7.5, 150 mM NaCl, 0.1% Tween) containing 5% non-fat dried milk. Finally, the membranes were probed with an appropriate dilution (1:500 to 1:2000) of primary antibody in TBST containing 5% non-fat dried milk for 1–4 h, depending upon the antibody.

Anti-caspase-3 antibodies from mouse, rabbit and goat were purchased from Transduction Laboratories, Inc., Upstate Biotechnology, Inc. and Santa Cruz Biotechnology, Inc., respectively.

The blots were washed three times for 1 h with TBST, followed by incubation in a peroxidase-coupled secondary antibody for 1 h in TBST containing 5% non-fat dried milk. The mouse, human, and rabbit peroxidase-coupled secondary antibodies were from Amersham. Enhanced chemiluminescence detection of the proteins was carried out using Hyperfilm ECL (Amersham), and with Pierce Super-Signal Substrate Western Blotting reagents, or Amersham ECL reagents.

2.5. Mitochondrial swelling assays

Rat liver mitochondria were prepared as described above. The peptide concentrations used to swell mitochondria were 50 μM L-SP, 10 μM D-(LSLARLATARLAI) (negative control), or 200 μM Ca^{+2} (positive control). The swelling was quantified by measuring the optical absorbance at 540 nm.

2.6. Activity of SP on fibroblasts

10^4 human embryonic kidney 293 cells per well were seeded into a 96-well plate. After 20 h, different aqueous dilutions (Fig. 2B) of SP (Sigma, USA), C31 and a peptide used as a control were added to the culture and the cell death was quantified by trypan blue exclusion 48 h later.

2.7. Toxicity of SP for bacterial cells

DH5α Escherichia coli cells were grown overnight as a pre-inoculum for the bacterial culture used in this assay. When the cells were at the end of their log phase (optical density at 600 nm of 0.8–1.0), 1 μl was used to inoculate 5 ml. Such dilution produced initial concentrations of bacteria capable of forming 10^5–10^6 colonies per ml in LB plates at 37°C, that is 10^5–10^6 colony forming units. All the bacterial cultures used in these experiments were grown in LB at 37°C. The concentration of SP required to inhibit the cell growth by 60% was determined by following bacterial growth in LB liquid in the presence of varying concentration of the peptide: 0, 1, 10, 20, 50, 125, and 250 μM. Sterilized 96-well plates of polystyrene with flat bottom and low evaporation lid (Costar, USA) were used, in a final volume of 100 μl: 50 μl of LB containing 10^5–10^6 colony forming units, and 50 μl of LB with a 2-fold dilution of the peptide. A 10 mM stock solution of the peptide was prepared with 5 mg of SP in 371 μl of water. Inhibition of growth was detected by measuring optical density at 600 nm with a microplate spectrophotometer SPECTRAmax (Molecular Devices,

USA) at varying times: 0, 3, 5, 6, 7 and 8 h. Each IC_{60} was determined from at least two independent experiments performed in triplicate. Additionally, the colonies formed from each experiment were counted in LB plates at 0 and 8 h of growth.

3. Results

The antibacterial peptides analyzed and biophysical properties previously determined are presented in Tables 1 and 2A, respectively.

In order to reproduce these biophysical properties, we calculated three scores from the sequences of these peptides. Table 2A shows a subset of selected antibacterial peptide sequences (see Section 2) and the corresponding experimental values for helix formation in water and in hydrophobic environments, antibacterial activity and cytotoxic activities against mammalian cells. Table 2B shows the corresponding calculated values for M, IP, A and the TI. We observed that the antibacterial peptides presented in Table 1 are more potent against G(−) (MIC = 17.3 μg/ml on average) bacteria than to G(+) (MIC = 44.3 μg/ml), and we used the G(−) values as a reference for the TI.

Peptide sequences with values ranging from $0.4 < M < 0.6$, $A < 10.0$ and $10.8 < IP < 11.7$, were found to have the highest TI (highest specificity for bacteria) (Table 2B). These parameters were therefore hypothesized to be the signature of the PAPs. Searching for PAPs in the SwissProt database led us to identify 14 PAPs (Table 3). Two of these peptides have previously been characterized with respect to their toxicity against bacteria and mammalian cells, and in both cases a greater toxicity towards bacterial cells was observed (Table 3).

3.1. Swelling of mitochondria and activation of caspase-3 by SP

One of the PAPs identified, SP, was tested for its ability to swell mitochondria and induce caspase-3 activation in a cell-free system. This system was developed previously in our group to simulate neuronal apoptosis (see Section 2 and [14]). We observed that SP induces the swelling of mitochondria at 50 μM in our system (data not shown). At such concentration, SP was capable of releasing cytochrome c from mitochondria and activating caspase-3 (Fig. 1). In contrast, a peptide chosen as negative control (see Section 2) which did not present the properties of PAPs (data not shown) did not display any observable effect on mitochondria (Fig. 1).

3.2. TI of SP

The toxicity of SP against bacteria was tested and compared to the effect of SP on fibroblasts when applied extracellularly. SP was able to reduce the growth of E. coli cells with an IC_{60} of 10 μM (Fig. 2B). By comparison, the negative control peptide did not have any toxicity against bacteria. In contrast, Fig. 2A shows that SP did not affect the growth of fibroblasts when applied extracellularly even at a concentration of 1 mM. These results indicate that SP has a TI > 100. Additionally, a peptide from the protein APP (the last 31 amino acids in APP, referred as C31) known to induce apoptosis when expressed intracellularly [16] was tested for its toxicity against bacteria and mammalian cells. This peptide did not present the properties (IP, M, A scores) of PAPs (data not shown). C31 did not present any observable toxicity against bacterial or mammalian cells when applied extracellularly (Fig. 2A,B).

Table 1
Peptide sequences of a subset of antibacterial peptides

Peptide name	Peptide sequence
(KIAKKIA)2NH2	KIAKKIAKIAKKIA-NH2
(KIAKKIA)3NH2	KIAKKIAKIAKKIAKIAKKIA-NH2
(KIAKLAK)2NH2	KIAKLAKKIAKLAK-NH2
(KIAKLAK)3NH2	KIAKLAKKIAKLAKKIAKLAK-NH2
(KALKALK)3NH2	KALKALKKALKALKKALKALK-NH2
(KLGKKLG)3NH2	KLGKKLGKLGKKLGKLGKKLG-NH2
CecropinA	KWKLFKKIEKVGQNIRDGIIKAGPAVAVVGQATQIAK-NH2
Melittin	GIGAVLKVLTTGLPALISWIKRKRQQ-NH2
Magainin 2	GIGKFLHSAKKFGKAFVGEIMNS-NH2
CA(1–13)M(1–13)NH2	KWKLFKKIEKVGQGIGAVLKVLTTGL-NH2
CA(1–8)M(1–18)NH2	KWKLFKKIGIGAVLKVLTTGLPALIS-NH2
Kla1	KLALKLALKAWKAALKLA-NH2
Kla2	KLALKAALKAWKAAAKLA-NH2
Kla3	KLALKAAAKAWKAAAKAA-NH2
Kla7	KAIAKSILKWIKSIAKAI-NH2
Kla8	KALAALLKKWAKLLAALK-NH2
Kla9	KLLAKAALKWLLKALKAA-NH2
Kla10	KALKKLLAKWLAAAKALL-NH2
Kla11	KITLKLAIKAWKLALKAA-NH2
Kla12	KALAKALAKLWKALAKAA-NH2
m2a	GIGKFLHSAKKFGKAFVGEIMNS-NH2
W16-m2a	GIGKFLHSAKKFGKAWVGEIMNS-NH2
L2R11A20-m2a	GLGKFLHSAKRFGKAFVGEAMNS-NH2
I6L15-m2a	GIGKFIHSAKKFGKLFVGEIMNS-NH2
I6A8L15I17-m2a	GIGKFIHAAKKFGKLFIGEIMNS-NH2
I6R11R14W16-m2a	GIGKFIHSAKRFGRAWVGEIMNS-NH2
I6V9W12T15I17-m2a	GIGKFIHSVKKWGKTFIGEIMNS-NH2
100-m2a	GIAKFGKAAAHFGKKWVGELMNS-NH2
140-m2a	GIGKFLHTLKTFGKKWVGEIMNS-NH2
160-m2a	GIGHFLHKVKSFGKSWIGEIMNS-NH2

The amino acids in the peptide sequence are represented in a one-letter code.

Table 2A
Observed characteristics of a subset of antibacterial peptides

Peptide	CD Water	Observed lipid	Antibacterial Gram(−)	Activity Gram(+)	Cytotoxicity	Reference
(KLAKKLA)2NH2	< 5	24	6	6	> 272	[8]
(KLAKKLA)3NH2	< 5	79	4	4	> 11	[8]
(KLAKLAK)2NH2	< 5	37	6	6	> 517	[8]
(KLAKLAK)3NH2	< 5	79	4	4	> 9	[8]
(KALKALK)3NH2	< 5	67	4	8	11	[8]
(KLGKKLG)3NH2	< 5	33	4	4	> 393	[8]
Cecropin A	0	75	0.2	> 300	> 200	[24]
Melittin	0	75	0.8	> 0.2	> 400	[24]
Magainin 2	0	44	4	300	300	[24]
CA(1–13)M(1–13)NH2	0	55	0.5	2	> 200	[24]
CA(1–8)M(1–18)NH2	0	63	0.3	1	> 600	[24]
Kla1	ND	73	5.2	2.6	11	[25]
Kla2	ND	68	11	45	107	[25]
Kla3	ND	59	91	> 91	> 200	[25]
Kla7	ND	70	5.6	1.4	1.8	[25]
Kla8	ND	62	5.8	3	2.5	[25]
Kla9	ND	55	6.2	1.6	1.7	[25]
Kla10	ND	62	6.1	1.5	2	[25]
Kla11	ND	69	5.3	5.3	10	[25]
Kla12	ND	67	6	1.5	10	[25]
m2a	ND	57	40	> 80	428	[25]
w16-m2a	ND	57	40	> 80	509	[25]
l2r11a20m2a	ND	45	75	> 75	> 100	[25]
i6l15-m2a	ND	57	38	38	260	[25]
i6a8l15i17m2a	ND	61	2.4	9.6	32	[25]
i6r11r14w16m2a	ND	52	37.5	> 75	303	[25]
i6v9w12t15i17-m2a	ND	64	2.3	18	56	[25]
100-m2a	ND	48	75	> 75	700	[25]
140-m2a	ND	75	13	13	35	[25]
160-m2a	ND	54	19	76	82	[25]

Peptide: see Table 1 for the amino acid composition for each peptide described in this table. CD Observed in water or lipid: percent of α-helical secondary structure determined by circular dichroism. Antibacterial activity G(+) or G(−): the minimal inhibitory concentration (μg/ml) for each peptide against Gram(+) and Gram(−) bacterial cells. Cytotoxicity: the concentration (μg/ml) required for inhibiting the growth of mammalian cells, usually red blood cells or fibroblasts.

4. Discussion

In order to optimize our homing pro-apoptotic approach to target and kill angiogenic endothelial cells supplying cancer cells, we have developed APAP, an approach to detect PAPs. APAP was originally developed to overcome the problems of toxicity and synthesis associated with our chemotherapeutic approach [1]. Positively charged PAPs, which are non-toxic outside the cell, are targeted to tumor vasculature by a fusion with a peptide that recognizes a receptor on the cell surface [17,18] and consequently internalized where they disrupt the negatively charged mitochondria, thereby exerting their pro-apoptotic effect.

We calculated the amphipathicity, IP and AGADIR scores for a subset of 30 different antibacterial peptides. The values grouping those peptides with the highest TI were considered the signature of PAPs. We searched for PAPs that resemble antibacterial ones, based on the posited relationship between mitochondrial-dependent apoptosis mechanisms and antibacterial activity. APAP provided us with a tool to identify PAPs independently of any sequence similarity with other known antibacterial or pro-apoptotic peptides. Additionally, APAP allowed us to search sequence databases systematically.

We calculated the amphipathicity and IP because amphipathic peptides are known to be membrane-associated [11], and the selectivity for recognizing bacterial-like membranes depends on the composition of the membranes [2,3]. Additionally, it has been previously recognized that hydrophobic peptides display both antibacterial activity and toxicity

against mammalian cells [19] (i.e. non-selective toxicity), thus PAPs would be expected not to be simply highly hydrophobic peptides. We observed that in our group of peptides (Table 1), all of the peptides but one were hydrophilic, constituting an appropriate group of peptides from which to select PAPs. It has been shown previously that antibacterial peptides with lower hydrophobicity display higher specificity towards Gram-negative bacteria [20]. In agreement with this notion, all the peptides analyzed in our study presented higher specificity towards G(−) bacteria as expressed by the TI values (Tables 2A and 2B).

Alternatively, the propensity to form soluble structures in water (expressed by the propensity to form secondary struc-
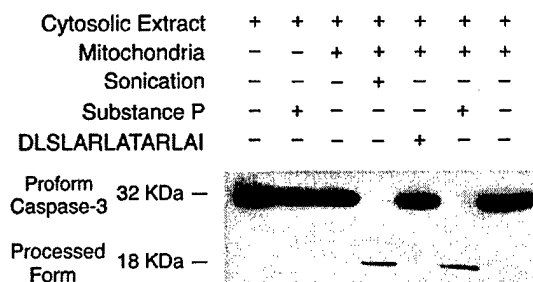

Fig. 1. Pro-apoptotic activity of SP. The release of cytochrome c from mitochondria and the processing of caspase-3 into the active form are shown for SP and controls (sonication, the detergent Triton X-100 and a non-toxic peptide DLSLARLATARLAI).

Table 2B
Calculated characteristics of a subset of antibacterial peptides

Peptide	A	M	IP	⟨H⟩	TI
(KLAKKLA)2NH2	4.5	0.48	11.5	−0.249	45.3
(KLAKKLA)3NH2	16.2	0.48	11.7	−0.249	2.8
(KLAKLAK)2NH2	5.1	0.48	11.5	−0.249	86.2
(KLAKLAK)3NH2	17.2	0.48	11.7	−0.249	2.3
(KALKALK)3NH2	16.6	0.48	11.7	−0.249	2.8
(KLGKKLG)3NH2	1.1	0.49	11.7	−0.274	98.3
Cecropin A	1.2	0.44	11.2	−0.123	1000.0
Melittin	3.1	0.46	12.6	−0.83	500.0
Magainin 2	0.8	0.56	10.8	−0.036	75.0
CA(1–13)M(1–13)NH2	1.1	0.53	11.1	−0.46	400
CA(1–8)M(1–18)NH2	1.3	0.43	11.4	0.065	2000
Kla1	13.4	0.16	11.4	−0.025	2.1
Kla2	10.6	0.30	11.4	−0.056	9.7
Kla3	7.2	0.17	11.4	−0.087	2.2
Kla7	2.4	0.53	11.4	−0.026	0.3
Kla8	49	0.51	11.4	−0.025	0.4
Kla9	18	0.38	11.4	−0.025	0.3
Kla10	23.5	0.45	11.4	−0.025	0.3
Kla11	14.8	0.16	11.4	−0.027	1.9
Kla12	19.5	0.49	11.4	−0.056	1.7
m2a	0.8	0.56	10.8	−0.036	10.7
w16-m2a	0.9	0.49	10.8	−0.046	12.7
12r11a20-m2a	0.9	0.51	11.1	−0.094	13.3
i6l15-m2a	0.6	0.54	10.8	−0.095	6.8
i6a8l15i17-m2a	1.1	0.55	10.8	0.016	13.3
i6r11r14w16-m2a	0.8	0.48	11.7	−0.095	8.1
i6v9w12t15i17-m2a	0.7	0.56	10.8	−0.035	24.3
100-m2a	1.1	0.46	10.8	−0.045	9.3
140-m2a	0.9	0.57	10.8	−0.049	2.7
160-m2a	0.7	0.57	10.5	−0.017	4.3

Peptide: see Table 1 for the amino acid composition for each peptide described in this table. A: AGADIR score. M: average helical hydrophobic moment. IP: estimated isoelectric point. ⟨H⟩: averaged hydrophobicity. TI: calculated therapeutic index.

tures in water, AGADIR score) was used in our approach. Since hydrophobicity and the propensity to form soluble structures in water are inversely related, it is expected that hydrophobic sequences will display a low AGADIR score. The inverse is not necessarily true, though; that is, peptide sequences with low AGADIR scores are not necessarily hydrophobic. Interestingly, PAPs tend to be hydrophilic with low AGADIR scores (Tables 2B and 3).

The peptides used to define the parameters of the PAPs (Table 1) are mostly synthetic peptides, with the exception of three natural peptides (magainin, cecropin A and melittin). None of these three natural peptides in Table 1 were detected

in our analysis because they were deposited in the SwissProt database in their mature form. In this form, they were longer than the cut-off value used to define the peptide database analyzed in this study (see Section 2 for a description of the peptide database used in this study). Alternatively, two cecropins (cec4_bommo, cecb_antpe) and two other natural antibacterial peptides (crbl_vescr, dms3_physa) were found in our search. In agreement with our predictions, these antibacterial peptides have been reported to have TIs similar to PAPs (Table 3). As further evidence of the validity of our approach, we tested two peptides, C31 and a control, that did not match the IP, M and A scores of PAPs (Fig. 2). The C31 peptide has

Table 3
PAPs in the SwissProt database

SwissProt name	A	M	IP	⟨H⟩	Length	Antibacterial activity Gram(−)	Cytotoxicity	Reference
Boll_megpe	7.9	0.52	11.1	0.058	17			
Cec4_bommo	0.5	0.44	11.3	−0.097	35			
Cecb_antpe	0.5	0.43	11.5	−0.132	35			
Crbl_vescr	0.7	0.50	11.6	0.144	13	15	>120	[24]
Dms3_physa	1.7	0.44	11.1	−0.024	30	2.5	80	[26]
Grar_ranru	0.04	0.53	11.6	−0.084	12			
Ranr_ranru	1.3	0.44	11.6	−0.239	17			
Npf_arttr	4.3	0.45	10.9	−0.297	36			
sp5m_bacsu	2.5	0.55	11.4	−0.095	26			
Stp_bpt4	1.7	0.43	11.1	−0.278	26			
Tkna_gadmo	0.03	0.48	11.6	−0.190	11			
Tkna_horse	0.03	0.51	11.6	−0.201	11			
Tkna_oncmy	0.01	0.49	11.6	−0.175	11			
Tkna_scyca	0.03	0.49	11.6	−0.124	11			

SwissProt name: the accession name in the SwissProt database for that particular peptide. A: AGADIR score. M: average helical hydrophobic moment. IP: calculated isoelectric point. ⟨H⟩: averaged hydrophobicity. Cytotoxicity: the concentration (μg/ml) required for inhibiting the growth of mammalian cells, usually red blood cells or fibroblasts.
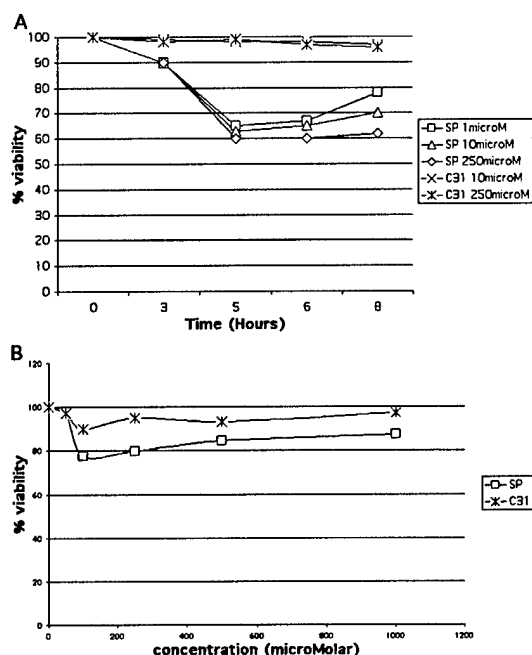
Fig. 2. Selective toxicity of SP on bacteria. The effect of SP and C31 on cell viability was measured on fibroblast cells (A) and bacteria cells (B). The viability is reported relative to a control (peptide DLSLARLATARLAI).

been shown to induce apoptosis by an unknown mechanism [16], so we considered it an interesting target for our study since we might provide some hints on the mechanism of action of C31 in addition to testing our approach. We found that none of these peptides is toxic to bacterial or mammalian cells when applied extracellularly thus confirming our predictions. Based on these results we propose that C31 may induce apoptosis by a different mechanism than PAPs.

In total, 14 sequences were identified as PAPs in the Swiss-Prot database (see Section 2). These 14 peptides can be placed into four different groups based on their known function; i.e. antibacterial peptides, neuropeptides, mast cell degranulating peptides and protein–protein interacting peptides. Two out of these four groups, antibacterial peptides and neuropeptides, represent more than 80% of the total (Table 3). Neuropeptides appear to be over-represented since there were only 48 neuropeptides in the original pool of 2473 peptides in the SwissProt database.

The special need for antibacterial peptides in the mammalian brain has been pointed out previously [21], since these may represent a more immediate line of control for bacterial infection than the immune system (which has a restricted access to the brain). Considering the properties of PAPs, our findings suggest that some previously identified neuropeptides may have antibacterial activity.

Among the neuropeptides identified as PAPs (Table 3), four were homologs of SP: tkna_gadmo, tkna_horse, tkna_oncmy, and tkna_scyca. SP belongs to the tachykinin family. Tachykinins are synthesized as larger protein precursors (usually more than 40 amino acids in length) that are enzymatically converted to their mature forms [22]. In our original search, we were able to detect only those recorded in the SwissProt

database in the active form. Analyzing all of the tachykinins deposited in the database (precursors and active forms), we found that 10 out of 61 were predicted to be PAPs (data not shown). Notably, these 10 were SP peptides from different species.

SP is known to form an α-helical structure in hydrophobic environments but not in aqueous solution [23], while it has a positive charge distribution over its sequence, supporting the finding that SP is a PAP. Therefore, the neuropeptide SP was tested for its preference for mitochondria-like membranes. The results presented in this work support our predictions that SP is a PAP. However, we did not observe a complete inhibition of *E. coli* growth, probably because of its well known short half-life in solution (minutes), while our experiments lasted for 8 h. Another possibility is that SP only displays a bacteriostatic activity, since the toxicity displayed by SP on bacterial cells was not markedly affected by the concentration of SP, as in the case of antibacterial peptides.

In developing APAP we focused on the characteristics that define selectivity rather than efficiency to kill bacteria. Therefore, it is not surprising that SP demonstrated bacteriostatic, but not bactericidal, activity. It is noteworthy that SP and most of the antibacterial peptides analyzed in this study (Table 1) are active in the low micromolar concentration range, and that SP is only 11 amino acids long. However, SP was toxic at higher concentrations than the antibacterial peptides in Table 1. We are currently working to use APAP to design more effective antibacterial peptides with higher TI values.

In conclusion, we have described a computational approach, APAP, to identify PAPs. These peptides display selectivity towards bacteria and mitochondria, with little toxic effect on eukaryotic cells when applied extracellularly, thus providing the basis for a new generation of drugs that can be present in the body without toxic effect unless they are taken in by targeted cells as we have shown previously [1]. From a public database, the approach detected mostly antibacterial peptides and neuropeptides suggesting that these neuropeptides may be the first reported with antibacterial activity. In agreement with this idea, we reported that SP is a PAP with a TI > 100. We speculate that these activities have been present in SP during the course of evolution of the tachykinins, which would support the possibility of a biological significance for these findings. APAP provides a method to detect and ultimately improve pro-apoptotic peptides for chemotherapy.

References

[1] Ellerby, H.M. et al. (1999) Nat. Med. 5, 1032–1038.
[2] Oren, Z. and Shai, Y. (1998) Biopolymers 47, 451–463.
[3] Matsuzaki, K., Sugishita, K., Fujii, N. and Miyajima, K. (1995) Biochemistry 34, 3423–3429.
[4] Hershberger, P.A., Dickson, J.A. and Friesen, P.D. (1992) J. Virol. 66, 5525–5533.
[5] Salvesen, G.S. and Dixit, V.M. (1997) Cell 91, 443–446.
[6] Zou, H., Li, Y., Liu, X. and Wang, X. (1999) J. Biol. Chem. 274, 11549–11556.
[7] Jurgensmeier, J.M., Xie, Z., Deveraux, Q., Ellerby, L., Bredesen,

D. and Reed, J.C. (1998) Proc. Natl. Acad. Sci. USA 95, 4997–5002.

[8] Javadpour, M.M., Juban, M.M., Lo, W.C., Bishop, S.M., Alberty, J.B., Cowell, S.M., Becker, C.L. and McLaughlin, M.L. (1996) J. Med. Chem. 39, 3107–3113.

[9] Oren, Z., Hong, J. and Shai, Y. (1999) Eur. J. Biochem. 259, 360–369.

[10] Munoz, V. and Serrano, L. (1994) Nat. Struct. Biol. 1, 399–409.

[11] Eisenberg, D., Weiss, R.M. and Terwilliger, T.C. (1984) Proc. Natl. Acad. Sci. USA 81, 140–144.

[12] Bairoch, A. and Apweiler, R. (1999) Nucleic Acids Res. 27, 49–54.

[13] Hovius, R., Lambrechts, H., Nicolay, K. and de Kruijff, B. (1990) Biochim. Biophys. Acta 1021, 217–226.

[14] Ellerby, H.M. et al. (1997) J. Neurosci. 17, 6165–6178.

[15] Moreadith, R.W. and Fiskum, G. (1984) Anal. Biochem. 137, 360–367.

[16] Lu, D.C. et al. (2000) Nat. Med. 6, 397–404.

[17] Pasqualini, R., Koivunen, E. and Ruoslahti, E. (1997) Nat. Biotechnol. 15, 542–546.

[18] Hart, S.L., Knight, A.M., Harbottle, R.P., Mistry, A., Hunger, H.D., Cutler, D.F., Williamson, R. and Coutelle, C. (1994) J. Biol. Chem. 269, 12468–12474.

[19] Kiyota, T., Lee, S. and Sugihara, G. (1996) Biochemistry 35, 13196–13204.

[20] Dathe, M., Wieprecht, T., Nikolenko, H., Handel, L., Maloy, W.L., MacDonald, D.L., Beyermann, M. and Bienert, M. (1997) FEBS Lett. 403, 208–212.

[21] Boman, H.G. (1995) Annu. Rev. Immunol. 13, 61–92.

[22] Maggio, J.E. (1988) Annu. Rev. Neurosci. 11, 13–28.

[23] Keire, D.A. and Kobayashi, M. (1998) Protein Sci. 7, 2438–2450.

[24] Argiolas, A. and Pisano, J.J. (1984) J. Biol. Chem. 259, 10106–10111.

[25] Lorenz, D., Wiesner, B., Zipper, J., Winkler, A., Krause, E., Beyermann, M., Lindau, M. and Bienert, M. (1998) J. Gen. Physiol. 112, 577–591.

[26] Mor, A., Hani, K. and Nicolas, P. (1994) J. Biol. Chem. 269, 31635–31641.

Targeting the prostate for destruction through a vascular address

Wadih Arap*†‡, Wolfgang Haedicke*†§, Michele Bernasconi*, Renate Kain¶‖, Daniel Rajotte*·**, Stanislaw Krajewski*, H. Michael Ellerby*††, Dale E. Bredesen*††, Renata Pasqualini*‡, and Erkki Ruoslahti*‡‡

*Cancer Research Center, The Burnham Institute, La Jolla, CA 92037; and ¶Department of Ultrastructural Pathology and Cell Biology, University of Vienna, A-1090 Vienna, Austria

Organ specific drug targeting was explored in mice as a possible alternative to surgery to treat prostate diseases. Peptides that specifically recognize the vasculature in the prostate were identified from phage-displayed peptide libraries by selecting for phage capable of homing into the prostate after an i.v. injection. One of the phage selected in this manner homed to the prostate 10–15 times more than to other organs. Unselected phage did not show this preference. The phage bound also to vasculature in the human prostate. The peptide displayed by the prostate-homing phage, SMSIARL (single letter code), was synthesized and shown to inhibit the homing of the phage when co-injected into mice with the phage. Systemic treatment of mice with a chimeric peptide consisting of the SMSIARL homing peptide, linked to a proapoptotic peptide that disrupts mitochondrial membranes, caused tissue destruction in the prostate, but not in other organs. The chimeric peptide delayed the development of the cancers in prostate cancer-prone transgenic mice (TRAMP mice). These results suggest that it may be possible to develop an alternative to surgical prostate resection and that such a treatment may also reduce future cancer risk.

D iseases affecting the prostate have gained major significance clinically and economically, primarily because of the increasing average age of the male population in the industrialized countries. Benign prostate hyperplasia affects to some degree most elderly men. Even more serious, the prostate is a frequent site of cancer. Some autopsy studies find that most men older than 70 have occult or overt cancer in the prostate (1). The surgical therapies of prostate hypertrophy and prostate cancer are associated with serious side effects, such as incontinence and impotence.

We have sought to develop a strategy that would provide a less traumatic treatment for prostate disease than is currently available. Our strategy is based on identification of peptides that home to specific sites in the vasculature by in vivo screening of intravenously injected phage libraries. These studies have revealed a surprising degree of specialization in the endothelia of various normal tissues (2, 3). Screening phage libraries for tumor homing has yielded a collection of peptides that home to tumor vasculature (4). We and others have used these tumor-homing peptides to direct therapies into tumors in mice (4, 5). We report here the identification of peptides that home to the vasculature of the prostate and the use of one of these homing peptides to deliver a proapoptotic peptide to the prostate.

Materials and Methods

Materials. Peptides were synthesized to our specifications by AnaSpec (San Jose, CA) or by our Peptide Synthesis Facility. The peptides were purified by HPLC and their identity was confirmed with mass spectrometry.

Apotag Kit for TUNEL staining was purchased from Intergen (Purchase, NY). Testosterone pellets (12.5 mg) and control pellets were from Innovative Research of America (Sarasota, FL), and controlled release pumps from Alzet (Mountain View, CA). The pumps were loaded with peptides following the manufacturer's instructions.

Mice. CD-1 male mice (The Jackson Laboratories) were used for phage screening at an age of 2–4 months. Transgenic adenocarcinoma of the mouse prostate (TRAMP) mice, kindly provided by Norman Greenberg, Baylor College of Medicine, Houston) were bred at our Animal Facility.

Phage Libraries and Library Screening. The phage libraries were prepared in the fUSE5 vector as described (6, 7). The primary library contains about 5×10^9 individual recombinant phage. For the library screening, CD-1 mice were anesthetized with Avertin (0.015 ml/g) and injected intravenously (tail vein) with phage libraries containing 10^9 transducing units diluted in 200 μl of DMEM. The phage was rescued from tissues by bacterial infection (2), and about 300 individual colonies were grown separately. The bacterial cultures were then pooled and the amplified phage were injected into mice as described above. To test individual phage for homing, 10^9 colony-forming units (cfu) (fUSE5) or 10^{10} plaque-forming units (pfu) (T7), diluted in 200 μl of PBS, were injected. The SMSIARL insert and its scrambled variant were cloned to the T7 phage (T7select415–1 vector; Novagen), and the resulting phage was tested as described (8).

Results

In vivo screening of a fUSE5 phage heptapeptide library for prostate-homing peptides (6) yielded two phage that accumulated selectively in the prostate. One of these phage, displaying the peptide SMSIARL (single letter code), homed to the prostate 15 times more than nonrecombinant control phage (Fig. 1a). The other prostate-selected phage (VSFLEYR) gave a prostate-homing ratio of ≈10. The homing of the SMSIARL phage to prostate tissue was inhibited when synthetic SMSIARL peptide was injected together with the phage, but not when an unrelated peptide was injected (Fig. 1a). The SMSIARL phage

MEDICAL SCIENCES

Fig. 1. Specific homing of phage to the prostate. (a) Phage selected for prostate homing accumulates specifically in the prostate and the homing is inhibited by soluble peptide. The SMSIARL fUSE5 phage, identified by *in vivo* screening, was tested for prostate homing. This phage and an irrelevant control phage were injected intravenously to male mice [10^9 colony forming units (cfu) per mouse] and the phage were rescued from various tissues based on their ability to infect a host bacteria. As indicated, 200 μg of the SMSIARL peptide or a control peptide (CARAC) was included in the injection to test inhibition of SMSIARL phage homing. (b) The SMSIARL peptide directs specific homing of T7 phage to the prostate. The SMSIARL sequence was cloned to the coat protein of the T7. A 1:10 mixture of SMSIARL and nonrecombinant control T7 phage [10^{10} plaque-forming units (pfu)] was injected and allowed to circulate for 7 min. Phage was extracted from prostate and brain with buffer (PBS), or a detergent solution (0.5% Nonidet P-40 in PBS) and plated, and 32 colonies were randomly chosen for PCR. The PCR products of SMSIARL and control phage DNA were distinguished on the basis of a size difference in a 4% agarose gel. (Control tissue was brain.)

homed also to the rat prostate tissue (not shown). The SMSIARL peptide when cloned into the T7 phage (6) showed a similar homing specificity for the prostate.

Phage displaying a scrambled variant of this peptide (LAM-SRIS) showed no homing to the prostate. The T7 SMSIARL phage was not enriched in the brain (Fig. 1b), salivary gland, kidney, testis, thymus, pancreas, skeletal muscle, or lung (not shown). We also confirmed the homing specificity by co-injecting

SMSIARL phage and nonrecombinant phage; the ratio of the two types of phage in the prostate was determined by PCR. The SMSIARL phage homed to the prostate 10–15 times more than the nonrecombinant phage. The recovery of the SMSIARL phage was more than 5-fold higher when the tissue was extracted with detergent rather than buffer alone. The brain as a control organ showed no enrichment with or without detergent (Fig. 1b). The greater phage recovery after lysis of the tissue with deter-
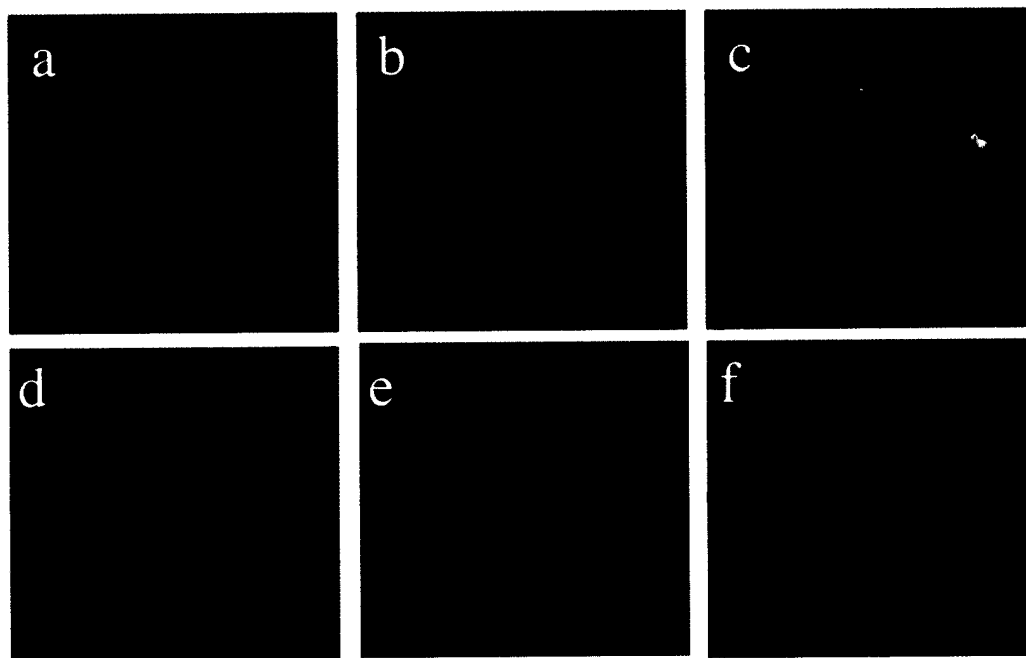
Fig. 2. Immunohistochemical staining of phage within prostate endothelial cells after i.v. injection into mice. SMSIARL-phage preparation was injected intravenously into mice. After 7 min circulation, animals were perfused with PBS, the prostate (*a–c*), brain (*d–f*), and various control organs were removed, processed for frozen sectioning, and stained with a polyclonal antibody against T7 phage (FITC; *a* and *d*) and CD31 (rhodamine; *b* and *e*). Merge with nuclear counterstain with DAPI (*c* and *f*). Control organs (kidney, spleen, lung; not shown) were negative for the phage, except for liver and spleen, where the reticuloendothelial tissue traps phage nonspecifically (4). (Magnification: ×400.)
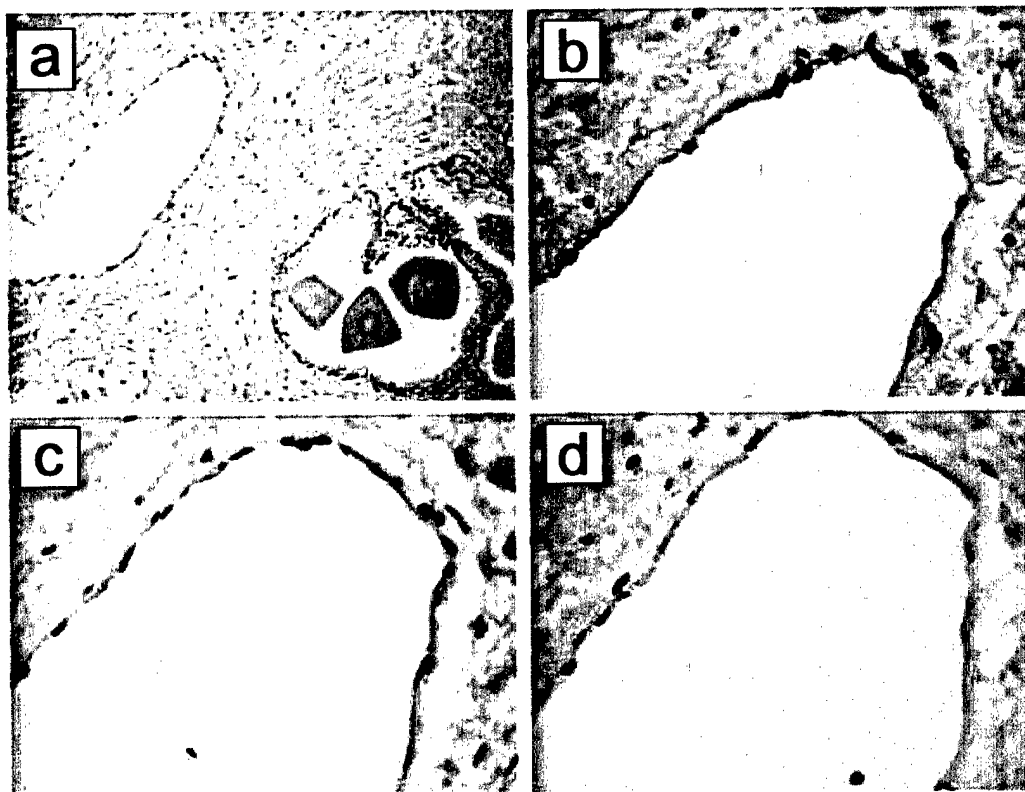
Fig. 3. SMSIARL phage binds to endothelium in human prostate. A human prostate tissue section containing both normal and cancerous tissue was overlaid with the SMSIARL phage (10^9 cfu/ml) and the binding of the phage was detected with anti-M13 phage antibody and peroxidase staining. (a) An overview ($\times 200$); (b) a detail from a at a higher magnification ($\times 400$). Staining of the endothelium is seen. (c) Overlay with phage that contains no peptide insert produces no endothelial staining. (d) The SMSIARL-phage staining is inhibited when soluble SMSIARL peptide is included in the overlay at 0.3 mg/ml.
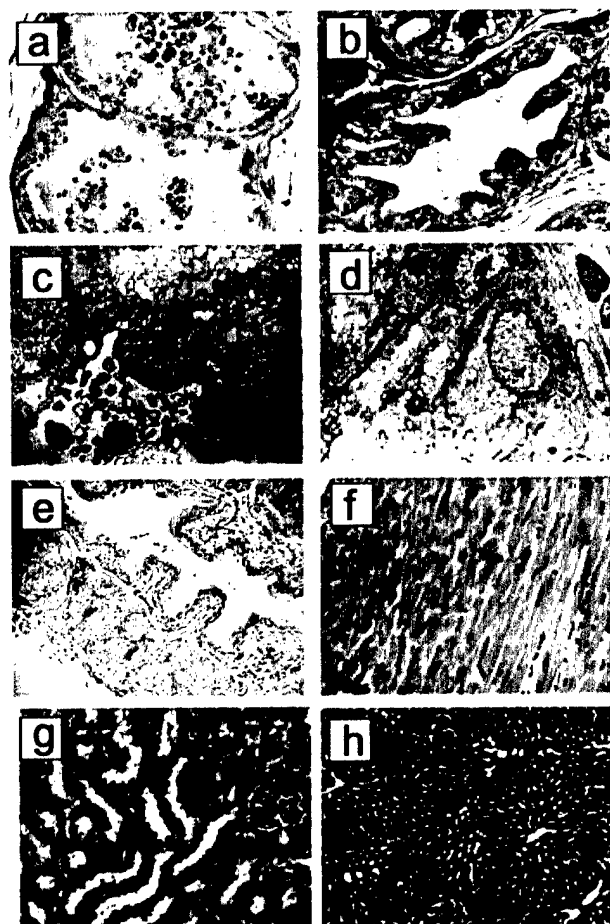
gent suggests that the SMSIARL phage may have been taken up into cells.

Antibody staining of the phage in tissue sections from mice injected intravenously with the T7 SMSIARL phage revealed staining in the prostate 7 min after an i.v. injection (Fig. 2). The phage staining colocalized with staining for the blood vessel marker CD31, indicating homing to blood vessels in the prostate. No specific staining was seen in control organs, or in prostate or control organs of mice injected with a nonrecombinant control phage. The phage staining appeared to be intracellular, supporting the detergent extraction results shown in Fig. 1b. Overlay of tissue sections from human prostate with the SMSIARL phage indicated that this phage also binds to the endothelium of human prostate blood vessels the same way it binds to the mouse prostate vessels (Fig. 3). Significantly, vessels in hypertrophic human prostate tissue bound the SMSIARL phage. No binding of this phage was detected in the blood vessels in several other human tissues. Similar localization results were obtained with the free SMSIARL peptide coupled to fluorescein (data not shown).

We next studied the ability of the SMSIARL peptide to deliver a biologically active compound to the prostate. $_D$(KLAKLAK)$_2$ is an amphipathic D-amino acid peptide that binds selectively to bacterial, but not eukaryotic cell membranes (9). It has antibacterial activity, but is relatively nontoxic to eukaryotic cells. We have previously shown that $_D$(KLAKLAK)$_2$, if delivered into mammalian cells, disrupts mitochondria (mitochondrial membranes resemble those of bacteria), initiating apoptosis (10). Conjugated through a G-G linker to a homing peptide that
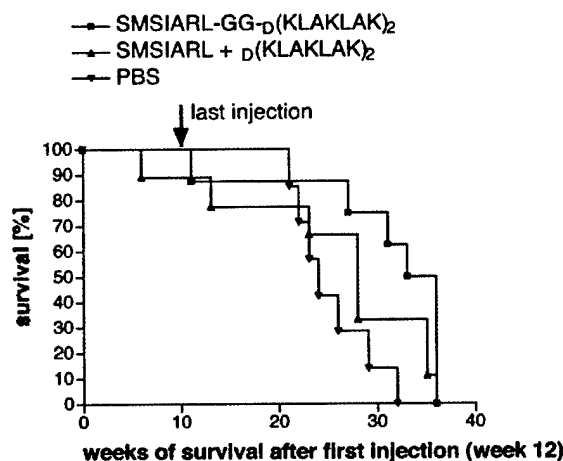
homes to tumor vasculature, $_D$(KLAKLAK)$_2$ yields a chimeric compound that is selectively cytotoxic to angiogenic endothelial cells and has antitumor activity *in vivo* (10). We used the same strategy to prepare a proapoptotic chimera that targets the vasculature of the normal prostate, and studied its ability to cause selective tissue destruction in the prostate.

Mice were injected with 250 μg of the targeted SMSIARL-GG-$_D$(KLAKLAK)$_2$ chimeric compound and the prostates were collected after 1, 4, 8, 12, 16, 24, and 48 h, and after 7 days. Control groups received $_D$(KLAKLAK)$_2$ coupled to a non-homing scrambled peptide (LAMSRIS), SMSIARL and $_D$(KLAKLAK)$_2$ as an uncoupled mixture, or buffer alone. A total of 62 mice treated with SMSIARL-GG-$_D$(KLAKLAK)$_2$ were evaluated. In prostates collected 16 h or later after the injection, histology revealed an unevenly distributed destruction of the prostate glandular epithelial cells that in some areas included epithelial shedding and destruction of entire glandular structures (Fig. 4a and b). These changes were still present 7 days after the treatment and no mitotic figures were observed, suggesting sustained damage and poor regeneration (not shown). Electron microscopy showed extensive destruction of intracellular organelles in the SMSIARL-GG-$_D$(KLAKLAK)$_2$-treated, but not control-treated, mice (Fig. 4 c and d). Tissue damage was also evident from an increase in TUNEL-positive vascular and glandular cell nuclei in the prostates of mice treated with SMSIARL-GG-$_D$(KLAKLAK)$_2$ (not shown). The prostates of control animals displayed only rare degenerating epithelial cells and all other organs examined (brain, heart, liver kidney, lung, urothelium) were histologically normal during or after treatment with each of the compounds (Fig. 4 e-h).

MEDICAL SCIENCES

Fig. 5. Survival of TRAMP mice treated with SMSIARL-GG-D(KLAKLAK)$_2$ or control materials. The treatment was initiated at 12 weeks of age. Male mice (ten per group) received i.v. injections of SMSIARL-GG-D(KLAKLAK)$_2$ peptide (200 μg per dose), or an equivalent dose of SMSIARL and (KLAKLAK)$_2$ as uncoupled peptides (control-treated group). The injections were given once a week for a total of ten doses. The mice in the SMSIARL-GG-D(KLAKLAK)$_2$ group survived significantly longer than the control mice treated with the uncoupled peptide mixture or with buffer.

Fig. 4. Targeted proapoptotic peptide to mouse prostate vasculature causes tissue damage in prostate but not in other tissues. Mice received an i.v. 250 μg injection of the SMSIARL-GG- D(KLAKLAK)$_2$ or an equivalent dose of SMSIARL and D(KLAKLAK)$_2$ as uncoupled peptides (control-treated mice). The mice were killed 24 h after the injection. Prostates were fixed in paraformaldehyde or glutaraldehyde solution and processed for light microscopy by staining with hematoxylin/eosin (H&E) or electron microscopy. Light microscopy showed focal loss of cell borders and epithelial shedding in the ventral lobe of prostates from the SMSIARL-GG- D(KLAKLAK)$_2$ group. (a) H&E-stained micrograph shows massive glandular destruction with nearly complete shedding of the glandular epithelial cells into the lumen. (b) A representative micrograph of normal prostate tissue from a mouse treated with the uncoupled peptide mixture. (Magnification in a and b, ×400.) (c) An electron microscopic image of a single epithelial cell from a SMSIARL-GG-D(KLAKLAK)$_2$-group prostate. The cell has sloughed off into the glandular lumen and massive destruction of its organelles is seen. (d) A representative micrograph of normal prostate shows intact cellular structure. (Magnification in c and d, ×6,000.) Light microscopy shows no damage to bladder (e; ×200), heart (f; ×400), kidney (g; ×400), or liver (h; ×400).

To effect sustained levels of the compounds used in the treatments, we used an implanted peristaltic pump for controlled release. Each pump was loaded with either SMSIARL-D(KLAKLAK)$_2$ or an uncoupled mixture of SMSIARL and D(KLAKLAK)$_2$. The animals were killed after 1 week, and their organs processed for histology. In another control experiment, we also implanted s.c. testosterone pellets to eliminate any variation in the sensitivity of prostate tissue caused by possible fluctuations in endogenous androgen levels (11). Seven days later, controlled release pumps loaded with the peptides were implanted on the peritoneal area opposite the pellets.

SMSIARL-GG-D(KLAKLAK)$_2$ consistently produced damage in the prostate (data not shown).

The tolerated dose of SMSIARLGG-D(KLAKLAK)$_2$ was limited by acute toxicity of the compound; the dose could be increased by giving the injection slowly over several minutes. Mice injected with SMSIARL-GG-D(KLAKLAK)$_2$, as well as those injected with equivalent amount of nonconjugated mixture of the homing peptide and proapoptotic peptide, showed marginal elevation of serum parameters of liver (ALT, AST, GGT) and kidney (creatinine and blood urea nitrogen) function. The levels returned to normal 1 week after the treatment. In one experiment, four mice that had been treated with four weekly injections of SMSIARL-GG-D(KLAKLAK)$_2$ were allowed to mate. Vaginal plugs showed that mating had occurred and litters were born in each case. These results suggest that SMSIARL-GG-D(KLAKLAK)$_2$ causes damage in the prostate, while other tissues are spared and the mice remain fertile.

We next analyzed the effect of a systemic SMSIARL-GG-D(KLAKLAK)$_2$ treatment on the longevity of TRAMP mice (12). Two independent experiments gave similar results; one of the experiments is shown in Fig. 5. The SMSIARL-GG-D(KLAKLAK)$_2$ survived significantly longer than the control groups that received the uncoupled peptides or buffer ($P < 0.01$ for both; Log Rank test).

Discussion

We show here that peptides selected from phage libraries for homing to the prostate vasculature reveal tissue-specific features in the blood vessels of the prostate. We also show that a peptide capable of homing to the blood vessels in the prostate can target a proapoptotic peptide to the prostate, and that systemic treatment with this targeted compound can cause destruction of prostate tissue and delay the development of prostate cancer in mice. Our results show that, like the vasculature of many other tissues analyzed in previous work (2–4), the vasculature of the prostate is biochemically distinct. The accumulation of the SMSIARL phage and fluorescein-labeled SMSIARL peptide in the prostate blood vessels after an i.v. injection indicates that this peptide binds selectively to the blood vessels in the prostate. The

selective destruction of prostate tissue caused by targeting of a proapoptotic peptide to the prostate with the SMSIARL homing peptide supports this conclusion.

The molecular nature of the vascular specialization is incompletely understood. We have identified the receptor for a peptide that homes to lung vasculature as membrane dipeptidase (13). Others have shown that a modified von Willebrand factor promoter is activated in endothelial cells in a tissue-specific manner under the influence of the surrounding parenchymal tissue (14), providing one possible regulatory mechanism for the expression of tissue-specific endothelial markers. Perhaps prostate tissue induces receptors for SMSIARL in the resident endothelium. Although the molecule the SMSIARL peptide binds to in the prostate vasculature remains to be identified, our results suggest some practical applications.

The destruction of prostate tissue by the SMSIARL-targeted proapoptotic peptide is likely to be secondary to loss of blood vessels, the main target of the homing peptide. However, we cannot exclude a direct effect on prostate epithelial cells. The tissue damage was specific for the prostate, suggesting that it may be possible to develop a "medical prostatectomy" procedure based on this principle. Such a procedure could provide an alternative treatment for prostate hypertrophy. Furthermore, the proapoptotic peptide treatment postponed the development of prostate cancer in TRAMP mice. We attribute the effect in the TRAMP mice to a reduction in the number of target cells available for malignant transformation, because the SMSIARL peptide does not home to the vessels in the TRAMP tumors (W.H. and E.R., unpublished result). The lifespan extension in our treated TRAMP mice was 6–8 weeks, close to 20% of the lifespan, even though the treatment works against a tremendous oncogenic pressure in these transgenic mice (12, 15). In human terms, this would mean postponement of prostate cancer development for several years. A medical treatment that reduces the size of the prostate and at the same time delays the development of prostate cancer could be an extremely useful procedure.

1. Cotran, R. S., Kumar, V. & Collins, T., eds. (1999) *Robbins Pathological Basis of Disease* (Saunders, Philadelphia), 6th Ed.
2. Pasqualini, R. & Ruoslahti, E. (1996) *Nature (London)* **380**, 364–366.
3. Rajotte, D., Arap, W., Hagedorn, M., Koivunen, E., Pasqualini, R. & Ruoslahti, E. (1998) *J. Clin. Inv.* **102**, 430–437.
4. Arap, W., Pasqualini, R. & Ruoslahti, E. (1998) *Science* **279**, 377–380.
5. Curnis, F., Sacchi, A., Borgna, L., Magni, F., Gasparri, A. & Corti, A. (2000) *Nat. Biotechnol.* **18**, 1185–1190.
6. Koivunen, E., Wang, B., Dickinson, C. D. & Ruoslahti, E. (1999) *Methods Enzymol.* **245**, 346–369.
7. Smith, G. P. & Scott, J. K. (1993) *Methods Enzymol.* **217**, 228–257.
8. Hoffman, J. A., Laakkonen, P., Porkka, K. & Ruoslahti, E. (2002) in *Phage Display, a Practical Approach*, eds. Lowman, H. & Clarkson, T. (Oxford Univ. Press, Oxford), in press.
9. Javadpour, M. M., Lo, W. C., Bishop, S. M., Alberty, J. B., Corwell, S. M.,

Becker, C. L. & McLaughlin, M. L. (1996) *J. Med. Chem.* **39**, 3107–3113.
10. Ellerby, H. M., Arap, W., Ellerby, L. M., Kain, R., Andrusiak, R., Del Rio, G., Krajewski, S., Lombardo, C. R., Ruoslahti, E., Bredesen, D. E. & Pasqualini, R. (1999) *Nat. Med.* **5**, 1032–1038.
11. Agus, D. B., Solde, D. W., Sgouros, G., Bellanzrud, A., Cordon-Cardo, C. & Scher, H. I. (1998) *Cancer Res.* **58**, 3009–3014.
12. Gingrich, J. R. Barrios, R. J., Morton, R. A., Boyce, B. F., DeMayo, F. J., Finegold, M. J., Angelopoulou, R., Rosen, J. M. & Greenberg, N. M. (1996) *Cancer Res.* **56**, 4096–4102.
13. Rajotte, D. & Ruoslahti, E. (1999) *J. Biol. Chem.* **274**, 11593–11598.
14. Aird, W. C., Edelberg, J. M., Weiler-Guettlez, H., Simmons, W. W., Smith, T. W. & Rosenberg, R. D. (1997) *J. Cell Biol.* **138**, 1117–1124.
15. Hsu, C. S., Ross, B. D., Chrisp, C. E., Derrowm S. Z., Charles, L. G., Pienta, K. J., Greenberg, N. M., Zeng, Z. & Sandor, M. G. (1998) *J. Urol.* **160**, 1500–1505.

MEDICAL SCIENCES

An Artificially Designed Pore-Forming Protein with Anti-Tumor Effects

H. Michael Ellerby[1]*, Sannamu Lee[2], Lisa M. Ellerby[1], Sylvia Chen[1], Taira Kiyota[2], Gabriel del Rio[1], Gohsuke Sugihara[2], Yan Sun[3], Dale E. Bredesen[1], Wadih Arap[3], & Renata Pasqualini[3]*

[1]*Program on Cancer and Aging, The Buck Institute, 8001 Redwood Blvd., Novato CA 94945, USA.*

[2]*Department of Chemistry, Faculty of Science, Fukuoka University, Jonan-ku, Fukuoka 814-80, Japan.*

[3] *The University of Texas M. D. Anderson Cancer Center, 1515 Holcombe Boulevard, Houston, TX 77030, USA*

* Corresponding authors
(e-mails: ellerby@buckcenter.org and rpasqual@notes.mdacc.tmc.edu)

SUMMARY

Protein engineering is an emerging area that has expanded our understanding of protein folding, and laid the groundwork for creation of unprecedented structures with unique functions. We previously designed the first native-like pore-forming protein, small globular protein (SGP). We show here that this artificially engineered protein has membrane-disrupting properties and anti-tumor activity in several cancer animal models. We propose and validate a mechanism for the selectivity of SGP towards cell membranes in tumors. SGP is the prototype for a new class of artificial proteins designed for therapeutic applications.

Running title: An artificially engineered protein with anti-tumor activity

Key words: protein engineering, SGP, anti-tumor, cancer therapy

INTRODUCTION

The tendency of amphipathic peptides to assemble in aqueous solution and of the β-turn to form a loop has been successfully employed to design coiled-coil proteins[4-6], various helix bundle proteins[7-12], and β-structural proteins[13,14]. *De novo* design of proteins with biological function, such as heme-binding, catalysis, or the formation of a membrane pore or channel, is perhaps the most challenging goal of peptide chemistry[3,15-21]. Much has been done recently in terms of designing membrane proteins that are correctly incorporated into membranes. However, relatively few attempts have been made to design proteins capable of disrupting membranes and subsequently causing cells death in vivo[21,22].

SGP is a 69 amino acid, 4-helix bundle protein, composed of 3 amphipathic helices, which consist of Leu and Lys residues and surround a single hydrophobic helix consisting of Ala residues, which create a pocket-like structure (Fig. 1A, B)[27,28]. SGP is monomeric in solution and denatures in a highly cooperative manner, characteristic of native globular-like proteins. SGP was conceived and designed based on the structure of the colicin family of bacteriocins[23-26]. While most naturally-occurring, pore-forming proteins maintain their tertiary structure when disrupting membranes, the colicins undergo a spontaneous transition from a native folded state in solution to an open umbrella-like state in membranes[23-26]. Nevertheless, SGP was designed to mimic this membrane insertion mechanism was confirmed in synthetic bilayers, where SGP formed a uniform size pore (14pS)[27]. It is still unknown whether or not SGP oligomerizes to form a channel.

Given that SGP forms pores in synthetic membranes, we asked whether it could disrupt biological membranes at the cellular level and whether it could be used successfully *in vivo* as an anti-tumor agent in vivo. We also investigated whether SGP would show any selectivity towards tumor cell lines in vitro and in vivo.

EXPERIMENTAL PROCEDURES

Reagents. SGP, SGP-L, and SGP-E were synthesized according to the Fmoc procedure starting from Fmoc-Leu-PEG [poly(ethylene glycol)] resin using a Miligen automatic peptide synthesizer (Model 9050) to monitor the deprotection of the Fmoc group by UV absorbance[27]. After cleavage from the resin by trifluoroacetic acid, the crude peptide obtained was purified by HPLC chromatography with an ODS column, 20 X 250 mm, with a gradient system of water/acetonitrile containing 0.1% trifluoroacetic acid. Amino acid analysis was performed after hydrolysis in 5.7 M HCl in a sealed tube at 110 °C for 24 hr. Analytical data obtained were as follows: Gly, 6.2 (6); Ala, 9.5 (10); Leu, 26.5 (25); Asp, 3.0 (3); Pro, 2.9 (3); Tyr, 3.1 (3); Lys, 18.9 (18). Molecular weight was determined by the FAB-mass spectrum using a JEOL JMX-HX100: base peak, 7555.1; calculated for $C_{367}H_{639}O_{77}N_{91} \bullet H^+$, 7554.8. Peptide concentrations were determined from the UV absorbance of Trp and three Tyr residues at 280 nm in buffer ($e = 8000$). Gel filtration HPLC chromatography was performed using Tris buffer (10 mM Tris, 150 mM NaCl, pH 5.0 or pH 7.4) on COSMOSIL 5DIOL-300 (Nakalai Tesk, Kyoto, Japan).

Computer model. The computer generated model of SGP was made with the program Insight II (Molecular Simulations Inc., San Diego, CA) running on an Octane SSE workstation (Silicon Graphics, Cupertino, CA).

Cell culture. All cell lines were obtained commercially. The Kaposi's sarcoma-derived cell line KS1767 and the breast carcinoma cell line MDA-MB-435 have been described previously[29-31] and were cultured in 10%FBS/DMEM, containing antibiotics.

4

Quantification of cell death. Cell viability was determined by morphology[29,30]. For viability assays, KS1767 cells were incubated with the concentrations of SGP, SGP (L), SGP (E), or control peptides indicated in the figures and in Table 1. Briefly, at the given time points, cell culture medium was aspirated from adherent cells. Cells were then gently washed once with PBS at 37°C. A 20-fold dilution of the dye mixture (100 μg/ml acridine orange and 100 μg/ml ethidium bromide) in PBS was then gently pipetted on the cells and viewed on an inverted microscope (Nikon TE 300). Cells with nuclei exhibiting margination and condensation of chromatin and/or nuclear fragmentation (early/mid apoptosis–acridine orange positive) or with compromised plasma membranes (late apoptosis–ethidium bromide positive) were scored as not viable; 500 cells per time point were scored in each experiment. Percent viability was calculated relative to untreated cells.

Human tumor xenografts. MDA-MB-435, KS1767, PC-3, and H358 derived human tumor xenografts were established in 2 month-old female or male (according to the tumor type), nude/nude Balb/c mice (Jackson Labs, Bar Harbor, ME) by administering 10^6 tumor cells per mouse in a 200 μl volume of serum free DMEM into the mammary fat pad or on the flank[29]. The mice were anesthetized with Avertin as described[29]. SGP was administered directly into the center of the tumor mass at a concentration of 100μM or 1 mM given slowly in 5 μl increments, for a total volume of 40 μl. Measurements of tumors were taken by caliper under anesthesia and used to calculate tumor volume[29]. Animal experimentation was reviewed and approved by the IACUC Committee.

Histology. MDA-MB-435-derived breast carcinoma and KS1767-derived Kaposi sarcoma xenografts and organs were removed, fixed in Bouin solution, embedded in paraffin for preparation of tissue sections, and stained with hematoxylin and eosin[29].

Skin toxicity. 2 month-old female nude mice (Jackson Labs, Bar Harbor ME) were

anesthetized with Avertin. 10 μl of 100 μM SGP or PBS was injected into the skin. The injected areas were monitored for 2 weeks.

Matrigel and cytotoxicity assays. Cell viability was determined by morphology[29,30]. KS1767 cells were incubated with SGP at 1 mM in the presence or absence of matrigel or polymeric fibronectin (sFN). The fibronectin polymer was produced as described[45]. Briefly, cell culture medium was aspirated from adherent cells. Cells were then coated with matrigel (gently pipetted on each well in order to completely coat the entire cell layer), or the fibronectin polymer, and incubated at 37°C for 10 minutes. SGP was added and the cells were viewed on an inverted microscope (Nikon TE 300). Cytotoxic assay in vitro and effects of matrigel. KS1767 cells were exposed to doxorubicin (20 μg/well) or SGP in the presence or absense of matrigel for 24 h. Cell viability (%) was evaluated after no treatment (medium or matrigel alone), incubation with SGP or doxorubicin. Cell death was evaluated morphologically[29,30] and cell viability was compared relative to untreated controls (no matrigel), or absence of SGP.

RESULTS

SGP effects on cultured cells.

To evaluate the effects of SGP on cell membranes we treated multiple human cell lines of different origins (Table 1). These lines included the Kaposi's sarcoma-derived cell line KS1767, the breast carcinoma-derived cell line MDA-MD-435, and the microvessel endothelial cell line DMEC[32,33]. Treatment of KS1767 cells with >10 μM SGP led to rapid cell death, characterized by 100% loss of viability within 60 seconds (Fig. 2A), as determined by Trypan Blue positivity. Such a rapid response suggests that the plasma membrane has been disrupted. Lowering the concentration of SGP to between 5 μM

6

and 10 μM led to induction of necrosis (scored morphologically), resulting in almost 100% loss of KS1767 cell viability over 60 min (Fig. 2B). SGP levels below 5 μM led to the induction of apoptosis over a 24-hour period (Fig. 2C), which was confirmed by a caspase-3 activation assay. KS1767 cells were unaffected by a 24 hour incubation in 100 μM of a control peptide (Fig. 2D). However, the classic morphological signs of apoptosis, such as nuclear condensation (Fig. 2E, short arrow) and plasma membrane blebbing (Fig. 2E, long arrow), were apparent in KS1767 cells after a 24-hour treatment with 3 μM SGP. Similar results were obtained using different cell lines, including several types of malignant cells (solid tumors and leukemic cell lines) and non-neoplastic cells (including endothelial cells and fibroblasts isolated from multiple organs and cells of glial origin, Table 1). As negative controls, we used altered forms of SGP (SGP-L and SGP-E). In SGP-L, the central all alanine helix was replaced by an all leucine helix. In SGP-E, the dimension of one of the helices has been altered, and we had previously determined that the ability of such analogs to disrupt synthetic membranes is diminished[28]. SGP-L and SGP-E were substantially less toxic to mammalian cultured cells (Table 1). The LC_{50} was increased by at least 10-fold in all cell types tested with SGP-L and SGP-E when these inactive versions of the protein were tested. These observations clearly show that the integrity of the SGP helices are required for SGP membrane disrupting activity. Taken together, these data demonstrate that SGP is a potent membrane-disrupting agent, but also that it is not selective and it will affect tumor derived cells as well as normal cells at similar concentrations (~3 μM).

SGP has anti-tumor activity *in vivo*.

Given the potent membrane-disrupting activity of SGP, we proceeded to evaluate SGP anti-tumor activity in nude mice bearing human tumor xenografts. We hypothesized that direct administration of SGP might reduce tumor volume and retard metastasis. In the first set of experiments, tumors were allowed to form after injection of a breast carcinoma cell line (MDA-MD-435), and then treated with local injections of SGP. We observed that tumor volume was significantly smaller in SGP treated mice than in the PBS treated control mice (Fig. 3A). Starting tumor volumes ranged from about 100 mm^3 to large sizes of about 600 mm^3. Tumor-bearing mice were given four weekly treatments of PBS, or 100 μM or 1 mM SGP (40 μl/treatment given in 5 μl increments). After a 4-week period without treatment, the tumor volumes were measured at 8 weeks. The average tumor volume at the end of the experiment in the SGP treated groups was 5 times less than the average volume seen in the PBS-treated group (Fig. 3A). There was no difference between the average tumor volumes of the 2 SGP treatment groups. Mice treated with SGP remained tumor-free for up to 4 months after tumor implantation, before being euthanized for histological evaluation. These observations indicate that both primary tumor growth and metastases were inhibited. Surgical examination of the tumor sites revealed no sign of tumor cells. Similar results were obtained when xenografts were produced by injection of prostate (Fig. 5A) and lung carcinoma (Fig. 5 B, C) cell lines. By successfully treating a large number of mice and testing the effects of SGP on several different tumor xenograft models (including carcinomas, sarcomas, and melanomas), we firmly established the therapeutic properties of SGP. Our data also show that that the anti-tumor effects of SGP are not limited to a specific tumor type. We also determined whether SGP produced adverse side effects such as necrosis when injected under normal skin. Strikingly, in all mice tested, SGP did not produce any surface effect when injected intradermally or sub-cutaneously (Fig. 3C) when compared with mice that did not receive the active form of SGP.

Histopathological analysis of SGP-treated MDA-MD-435 human breast carcinoma xenografts showed widespread cell death (Fig. 4B), as compared with PBS treated tumors (Fig. 4A). Many condensed nuclei were apparent (Fig. 4B, short arrows), and there was no effect on the extracellular matrix (Fig. 4B, long arrows). Apoptosis was confirmed by a caspase-3 activation assay (data not shown). It is noteworthy that while 100 μM SGP induced almost immediate cell death *in vitro* that was apparently neither apoptotic nor necrotic, 100 μM SGP induced apoptosis *in vivo*. Work is underway to evaluate lower concentrations. SGP treated human KS1767 Kaposi's sarcoma-derived xenografts showed similar effects (Fig. 4C,D). Histological analysis of the major organs of SGP treated mice showed no overt pathology, confirming that SGP treatments do not affect sites other than the injected tumor area (data not shown). Thus, SGP has anti "tumor" specific effects, without showing any "tumor cell" specific effects).

Mechanism of SGP action and selectivity towards cell membranes

To determine the mechanisms responsible for selective anti-tumor activity of SGP *in vivo*, we designed a matrigel assay (to mimic extracellular matrix). In the absence of matrigel, SGP led to severe disruption of cell membranes, resulting in almost 100% loss of viability over 10 min (Fig. 6B). In contrast, in the presence of matrigel, KS1767 cells were unaffected by incubation with 1 mM SGP (Fig. 6D). This loss of membrane disrupting ability in the presence of a thin matrigel layer could account for the lack of SGP toxicity seen *in vivo*. Ethanol, as shown in Fig. 6E, or cytotoxic drugs such as doxorubicin (Fig 7) damaged the cell layer under similar conditions, regardless of the presence of matrigel, which fails to provide protection from the other toxic agents because these other agents more readily diffuse through the matrix. When matrigel was

9

replaced by polymeric fibronectin (sFN)[45], another form of matrix, SGP was also ineffective and did not interfere with cell viability (Fig. 6 E) while ethanol induced massive cell death. Fibronectin alone did not prevent SGP activity and was used as a control.

The observations in this model are consistent with the lack of skin toxicity seen with SGP. We propose that the discrepancy between in vitro and in vivo SGP effects (anti-tumor cell activity versus selective anti-tumor activity) results from the potent membrane-disrupting activity of SGP, which is inactivated in the presence of ECM and connective tissue.

DISCUSSION

SGP represents an interesting class of anti-cancer proteins whose therapeutic effects can be optimized by amino acid substitution and by altering helical domain length and hydrophobicity[29,35]. Although SGP is a non-specific membrane-disrupting agent, it is selective in the sense that the disruption is limited *in vivo*. Unlike detergents, which solubilize membranes, SGP physically disrupts membrane architecture, leading to cell lysis. This explains the lack of SGP toxicity when the protein is injected sub-cutaneously or intradermally. Recently published data also suggest that the lipid membrane-disruption properties of SGP are responsible for the anti-tumor activity of the agent[28].

We report one of the first examples of a pore-forming peptide or protein, natural or synthetic, being applied successfully to treat established human tumor xenografts. It is important to emphasize that SGP is not a bacterial toxin, although such agents (or their natural or recombinant form) have been extensively explored as anti-cancer therapies[34]. Several pore-forming peptides and proteins have been shown to have moderate efficacy

in killing tumor cells *in vitro*, yet very limited anti-tumor effects were seen *in vivo*. The anti-bacterial peptides magainin (and synthetic derivatives),[37] cecropin (and synthetic derivatives),[38] granulysin,[39] and NK-lysin[40] are toxic to tumor cells in culture. The pore-forming protein verotoxin 1 (a colicin) has also been shown to have a toxic effect on tumor cells *in vitro*[41]. Magainin, cecropin and verotoxin 1 also had limited efficacy *in vivo* in mice bearing murine tumors[37,38,41].

Cytotoxic agents developed within the past few decades have been based on naturally existing compounds, synthetic peptides, or protein fragments representing active membrane-disrupting domains. In contrast to such compounds, SGP is a protein that was artificially created to perform a pre-determined biological function. Moreover, therapeutically significant cell membrane disrupting activity was observed *in vivo*.

SGP activity appears to be restricted to the presence of lipid bilayers in vitro, while in vivo its activity appears to be limited to tumors in vivo due to the protective effect of extracellular matrix components. In vitro, SGP shows no selectivity towards normal or malignant cells, under the experimental conditions tested. We show here that SGP is potentially a valid anti-cancer agent; applications include Kaposi's sarcoma, malignant melanoma of the skin, or palliation for unresectable or metastatic tumors in anatomical sites difficult to treat with other modalities. Moreover, SGP variants in which residues critical for helical structure are altered are inactive, suggesting that the structure of the protein is intrinsically linked to its ability to damage cell membranes. Although the *de novo* design of proteins with biological function is in its early stages, novel therapeutic strategies may may emerge from the activity of designed proteins such as SGP.

ACKNOWLEDGMENTS

REFERENCES

1. Klemba, M.W., Munson, M. & Regan, L. (1998) *Proteins: Analysis and Design.* (ed. Angeletti, R.H.) (Academic Press) **5**: 313-353.

2. Bryson, J.W., Betz, S.F., Lu, H.S., Suich, D.J., Zhou, H.X., O'Neil, K.T. & DeGrado, W.F. (1995) *Science* **70**: 935-941.

3. Tuchscherer, G., Scheibler, L., Dumy, P. & Mutter, M. (1998) *Biopolymers* **47**: 63-73.

4. DeGrado, W.F., Wasserman, Z.R. & Lear JD. (1989) *Science* **243**: 622-628.

5. Betz, S.F., Liebman, P.A. & DeGrado, W.F. (1997) *Biochemistry* **36**: 2450-2458.

6. Bryson, J.W., Desjarlais, J.R., Handel, T.M. & DeGrado, W.F. (1998) *Prot. Sci.* **7**: 1404-1414.

7. Walsh, S.T., Cheng, H., Bryson, J.W., Roder, H. & DeGrado, W.F. (1999) *Proc. Natl Acad. Sci. USA* **96**: 5486-5491.

8. Hecht, M.H., Richardson, J.S., Richardson, D.C. & Ogden, R.C. (1990) *Science* **249**: 884-891, 1990.

9. Dekker, N., Cox, M., Boelens, R., Verrijzer, C.P., van der Vliet, P.C. & Kaptein, R. (1993) *Nature* **362**: 852-855.

10. Zhou, N.E., Kay, C.M. & Hodges, R.S. (1992) *J. Biol. Chem.* **267**: 2664-2670.

11. Kamtekar, S., Schiffer, J.M., Xiong, H., Babik, J.M. & Hecht, M.H. (1993) *Science* **262**: 1680-1685.

12. Monera, O.D., Zhou, N.E., Lavigne, P., Kay, C.M. & Hodges, R.S. (1996) *J. Biol. Chem.* **271**: 3995-4001.

13. Quinn, T.P., Tweedy, N.B., Williams, R.W., Richardson, J.S. & Richardson, D.C. (1994) *Proc. Natl Acad. Sci. USA* **91**: 8747-8751.

14. Hecht, M.H. (1994) *Proc. Natl Acad. Sci. USA* **91**: 8729-8730.

15. Handel, T.M., Williams, S.A. & DeGrado, W.F. (1993) *Science* **261**: 879-885.

13

16. Lazar, G.A., Desjarlais, J.R. & Handel, T.M. (1997) *Prot. Sci.* **6**: 1167-1178.

17. Rojas, N.R., Kamtekar, S., Simons, C.T., McLean, J.E., Vogel, K.M., Spiro, T.G., Farid, R.S. & Hecht, M.H. (1997) *Prot. Sci.* **6**: 2512-2524.

18. Farinas, E. & Regan, L. (1998) *Prot. Sci.* **7**, 1939-1946.

19. Tommos, C., Skalicky, J.J., Pilloud, D.L., Wand, A.J. & Dutton, P.L. (1999) *Biochem.* **38**, 9495-9507.

20. Corey, M.J. & Corey, E. (1996) *Proc. Natl Acad. Sci. USA* **93**: 11428-11434.

21. Bayley, H. (1999) *Curr. Opin. Biotechnol.* **10**, 94-103.

22. Mingarro, I., von Heijne, G. & Whitley, P. (1997) Membrane-protein engineering. *Trends in Biotechnol.* **15**: 432-437.

23. Konisky, J. (1982) *Ann. Rev. Microbiol.* **36**: 125-144.

24. van der Goot, F.G., Gonzalez-Manas, J.M., Lakey, J.H. & Pattus, F. (1991) *Nature* **354**: 408-410.

25. Zakharov S.D., Lindeberg M., Griko Y., Salamon Z., Tollin G., Prendergast F.G. Cramer W.A. (1998) *Proc. Natl. Acad. Sci., USA* **95**:4282-4287.

26. Mel, S.F. & Stroud, R.M. (1993) *Biochem.* **32**: 2082-2089.

27. Lee, S., Kiyota, T., Kunitake, T., Matsumoto, E., Yamashita, S., Anzai, K. & Sugihara, G. (1997) *Biochem.* **36**: 3782-3791.

28. Matsumoto, E., Kiyota, T., Lee, S., Sugihara, G., Yamashita, S., Meno, H., Aso, Y., Sakamoto, H. & Ellerby, H.M. (2001) *Biopolymers* **56**: 96-108.

29. Ellerby, H.M., Arap, W., Ellerby, L.M., Kain, R., Andrusiak, R., Rio, G.D., Krajewski, S., Lombardo, C.R., Rao, R., Ruoslahti, E., Bredesen, D.E. & Pasqualini, R. (1999) *Nat. Med.* **5**: 1032-1038.

30. Ellerby, H.M., Martin, S.J., Ellerby, L.M., Naiem, S.S., Rabizadeh, S., Salvesen, G.S., Casiano, C.A., Cashman, N.R., Green, D.R. & Bredesen, D.E. (1997) *J. Neurosci.* **17**: 6165-6178.

31. Alnemri, E.S., Livingston, D.J., Nicholson, D.W., Salvesen, G., Thornberry, N.A., Wong, W.W. & Yuan, J. (1996) *Cell* **87**: 171.

32. Herndier, B.G., Werner, A., Arnstein, P., Abbey, N.W., Demartis, F., Cohen, R.L., Shuman, M.A. & Levy, J.A. (1994) *Aids* **8**: 575-581.

33. Reisbach, G., Gebhart, E. & Cailleau, R. (1982) *Anticancer Res.* **2**: 257-260.

34. Pastan, I., Chaudhary V., & FitzGerald D.J. (1992) *Ann. Rev. Biochem.* **61**: 331-354.

35. Dathe, M., Wieprecht, T., Nikolenko, H., Handel, L., Maloy, W.L., MacDonald, D.L., Beyermann, M. & Bienert, M. (1997) *FEBS Lett.* **403**: 208-212.

36. Brothman, A. (1997) *Encyclopedia of Cancer.* (ed. Bertino, J., Acad. Press), **2**, 1303-1313.

37. Ohsaki, Y., Gazdar, A.F., Chen, H.C. & Johnson BE. (1992) *Cancer Res.* **52**: 3534-3538.

38. Moore, A.J., Devine, D.A. & Bibby, M.C. (1994) *Peptide Res.* **7**: 265-269.

39. Gamen, S., Hanson, D.A., Kaspar, A., Naval, J., Krensky, A.M. & Anel, A. (1998) *J. Immunol.* **161**: 1758-1764.

40. Andersson, M., Gunne, H., Agerberth, B., Boman, A., Bergman, T., Sillard, R., Jornvall, H., Mutt, V., Olsson, B., Wigzell H., Dagerlind, A., Bowman, H.G. & Gudmundsson, G.H. (1995) *EMBO J.* **14**: 1615-1625.

41. Farkas-Himsley, H., Hill, R., Rosen, B., Arab, S. & Lingwood, C.A. (1995) *Proc. Natl Acad. Sci. USA* **92**: 6996-7000.

42. Kagawa, S., Gu, J., Swisher, S.G., Ji, L., Roth, J.A., Lai, D., Stephens, L.C. & Fang, B. (2000) *Cancer Res.* **60**: 1157-1161.

43. Pataer, A., Fang, B., Yu, R., Kagawa, S., Hunt, K.K., McDonnell, T.J., Roth, J.A., & Swisher, S.G. (2000) *Cancer Res.* **60**: 788-792.

44. Costantini, P., Belzacq, A.S., Vieira, H.L., Larochette, N., de Pablo, M.A., Zamzami, N., Susin, S.A., Brenner, C. & Kroemer, G. (2000) *Oncogene* **19**: 307-314.

45. Pasqualini, R., Bourdoulous, S., Koivunen, E., Woods, V. L., Jr., and Ruoslahti, E. (1996) *Nature Med.* **2**: 1197-203.

FIGURE LEGENDS

Table 1. **Comparative study of the properties of SGP and SGP mutants.**

Fig. 1. SGP representations and mechanism. A, Amino acid sequence of SGP. Hydrophobic leucine and alanine residues are shown in red, and positively charged lysine residues are in green. Loop residues (glycine, proline, and asparagine) are shown in blue, and tyrosine and tryptophan residues are in black. B, Helical wheel diagram of SGP. C, The putative mechanism of SGP. In the aqueous phase SGP folds into a globular protein (upper), but in lipid membranes it adopts an inverted umbrella-like structure forming a pore (lower).

Fig. 2. SGP treatment of cultured tumor cells. A, Human Kaposi's sarcoma derived KS1767 cells treated with 10 μM SGP undergo extremely rapid cell death within 60 sec (black bars), while those treated with 100 μM of negative control peptide DLSLARLATARLAI are unaffected (scheme bars) ($p < 0.04$). B, Decreased viability is observed in KS1767 cells treated with 10 μM SGP within 60 min (black bars), while those treated with 100 μM of negative control peptide are unaffected after 60 min (gray bars) ($p < 0.03$). C, No viable cells are observed after treatment with 3 μM SGP over 24 hrs, while cells treated with 100 μM of negative control peptide are unaffected after 24 hr (gray bars) ($p < 0.05$). Hoffman contrast microscopy of KS1767 cells treated with 100 μM of negative control peptide (panel D) for 24 hrs or 3 μM SGP for 24 hrs (panel E). Cells with nuclei exhibiting margination and condensation of chromatin and/or nuclear fragmentation (early/mid apoptosis–acridine orange positive) or with compromised plasma membranes (late apoptosis–ethidium bromide positive) were scored as not viable (500 cells per time point were scored in each experiment). Percent viability was

16

calculated relative to untreated cells under all experimental conditions. Classic morphological characteristics of cell death including condensed nuclei (short arrows) and plasma membrane blebbing (long arrows), are evident. Results were reproduced in three independent experiments.

Fig. 3. SGP treatment of nude mice bearing human breast cancer and Kaposi's sarcoma-derived xenografts. Data are shown for human MDA-MB-435-derived breast carcinomas. Mice had tumor volumes ranging from 100 mm^3 to 600 mm^3 and were divided in similar groups based on matched tumor volumes at the start of the experiment (open circles). A, SGP-treated tumors are smaller than controls (PBS-treated or SGP-treated tumor volumes at the end of the experiment are represented as closed circles). Differences in tumor volumes at 8 weeks are shown (*t* test, $P<0.05$). A total of 10 mice received SGP. B, Representative pictures of tumors after 4 weekly treatments with SGP at 40μl/week, n=5 for each experimental group. The volume of the PBS treated tumor is 400 mm^3 (left), while 100 μM SGP (middle) and 1mM SGP (right) treated tumors have flattened and virtually disappeared. These three tumors began at volumes of 100 mm^3. C, Lack of skin toxicity of SGP. Subcutaneous injection (40μl) of 100 μM SGP (left injection sight, arrow) and of PBS (right injection site, arrow) demonstrates that SGP is relatively non-toxic to normal skin. Results represented on C were reproduced in eight independent experiments.

Fig. 4. SGP-treated tumors undergo widespread cell death. Histopathological tissue sections of human tumor xenografts harvested at 8 weeks after treatment initiation are shown. Tissue sections from human MDA-MB-435-derived breast carcinoma xeno-grafts from nude mice treated with PBS-treated tumor tissue but with 100 μM SGP, show extensive apoptosis with many evident condensed nuclei (short arrows) and an intact extra-cellular matrix (long arrows); n=7 for each experimental group. Tissue sections from human KS1767-derived Kaposi's sarcoma xenografts in nude mice had a

similar outcome, a representative image of a PBS treated tumor and a tumor treated with SGP are shown.

Fig. 5. SGP treatment of nude mice bearing human prostate and lung cancer xenografts. Data are shown for human PC3-derived prostate carcinoma and H358 lung carcinoma. Tumor cells were implanted on the flank at the start of the experiments. Mice were divided in similar groups based on matched tumor volumes at the start of the experiment (open circles). A, SGP-treated PC-3 tumors are smaller than control PBS-treated tumors. Differences in tumor volumes at 10 weeks are shown (t test, $P<0.05$). B, SGP treated H358 tumors are smaller than control PBS treated tumors. Differences in tumor volumes at 9 weeks are shown (t test, $P<0.05$). C, representative pictures of tumors after 6 weekly treatments at 40μl/week (see Methods); n=7 for each experimental group. SGP- treated tumors, as indicated, have disappeared. A, SGP-treated tumors are smaller than controls (PBS-treated or SGP-treated tumor volumes at the end of the experiment are represented as closed circles).

Fig. 6. SGP treatment of cultured tumor cells in the presence or absence of matrigel or polymeric fibronectin. A, Treatment of KS 1767 cells with 1 mM SGP decreases cell viability and lead to condensed nuclei and plasma cell membrane blebbing, B, while cells treated with 1 mM of SGP in the presence of matrigel remain unaffected after 60 min, D. KS1767 cells without (A) or with a layer of matrigel, C, remained healthy for as long as 48 h. Results were reproduced in four independent experiments. E, KS1767 cells were exposed to SGP in the presence or absence of polymeric fibronectin. In contrast to cells exposed to ethanol, cells treated with 1 mM of SGP in the presence of polymeric fibronectin (sFN) remain unaffected (p<0.01, *). Cell viability (%) was evaluated morphologically. Shown are SEM obtained from triplicate wells. Results were reproduced in three independent experiments.

Fig. 7. Cytotoxic assay in vitro and effects of matrigel. KS1767 cells were exposed to doxorubicin or SGP in the presence or absence of matrigel for 24 h. Cell viability (%) was evaluated at 24 h after no treatment (medium or matrigel alone), or incubation with SGP or doxorubicin (20 µg/well), as indicated. In contrast to SGP, doxorubidin decreased cell viability ($p<0.01$, *) in the presence of matrigel. Shown are SEM obtained from triplicate wells. Results were reproduced in four independent experiments.

A

Ac-A-A-A-A-A-W-A-A-A-A-G-P-N-G-

L-Y-L-K-K-L-K-K-L-L-K-L-L-G-N-P-G-

L-K-L-Y-K-K-L-L-K-K-L-L-K-L-G-N-P-G-
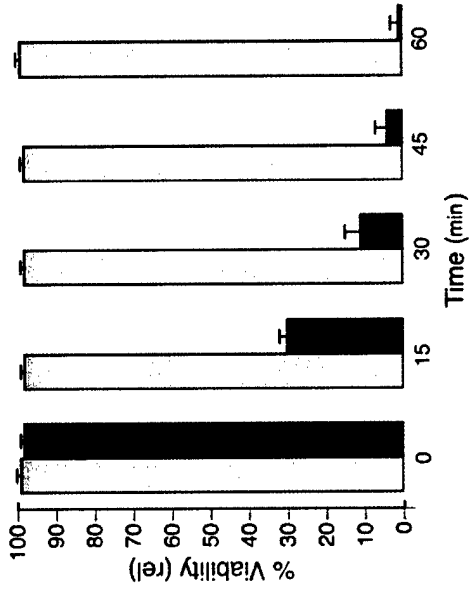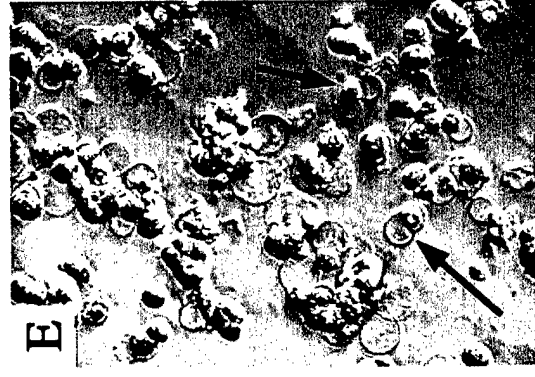
L-L-K-L-Y-K-K-L-L-K-K-L-L-K-L-L-OH

B

C

A

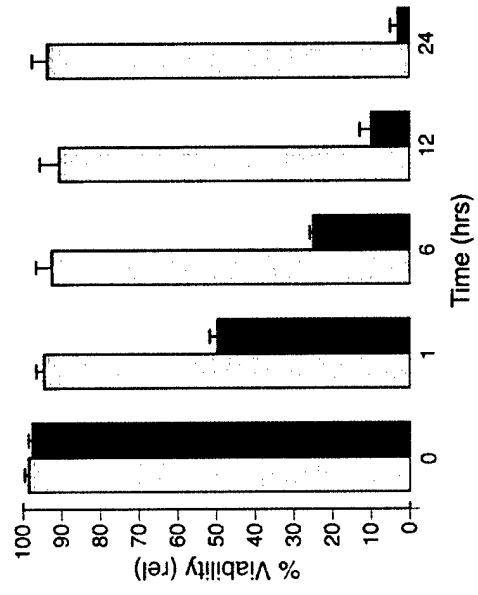% Viability (rel) vs Time (sec): 0, 15, 30, 45, 60

B

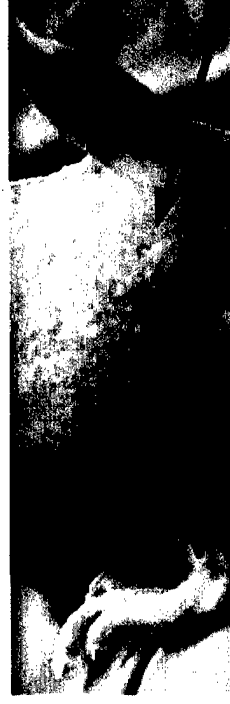% Viability (rel) vs Time (min): 0, 15, 30, 45, 60

C

% Viability (rel) vs Time (hrs): 0, 1, 6, 12, 24

D

E

A

Tumor Volume (mm³)
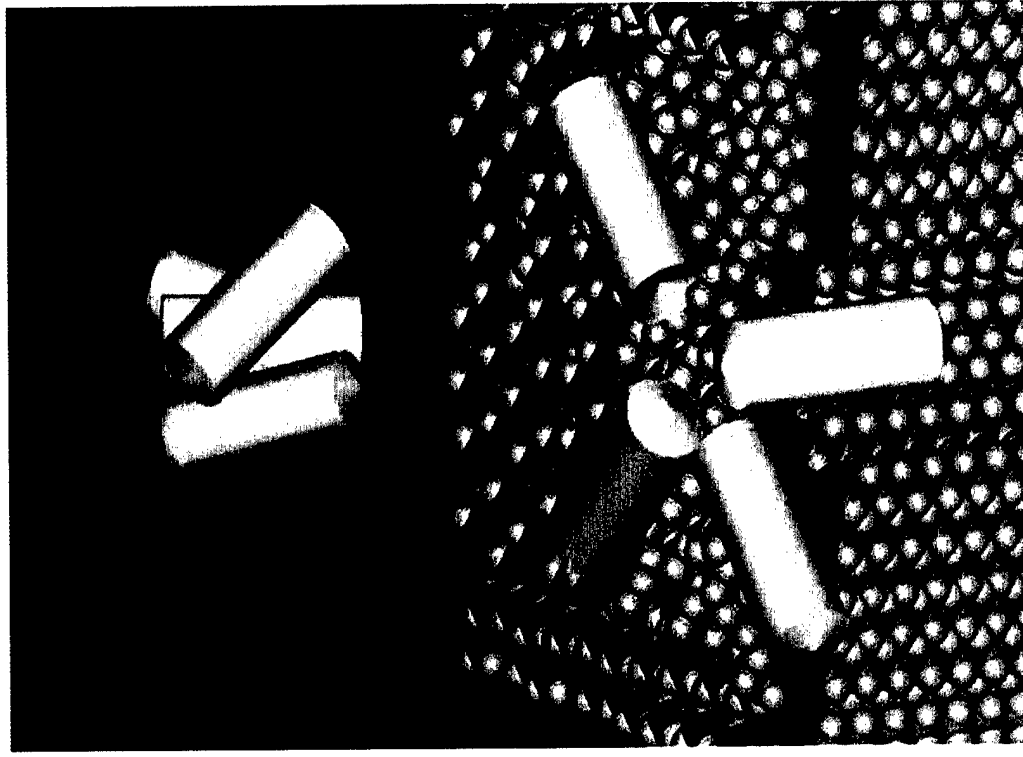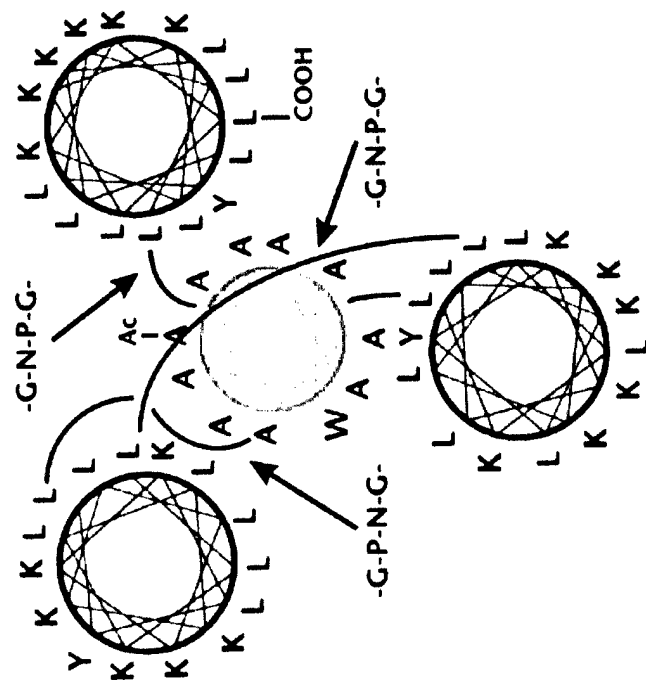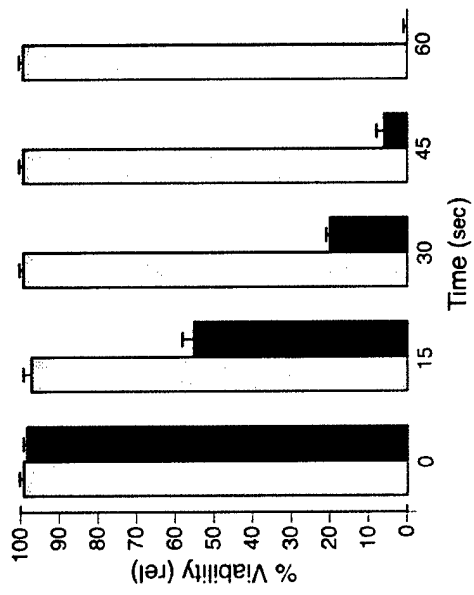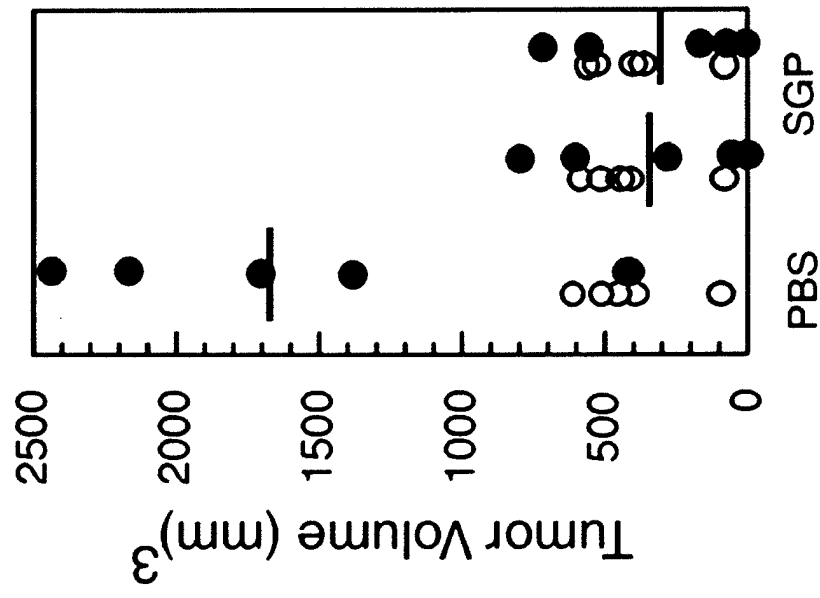
B

C

MDA-MB-435 Tumors

PBS

SGP

KS 1767 Tumors

PBS

SGP
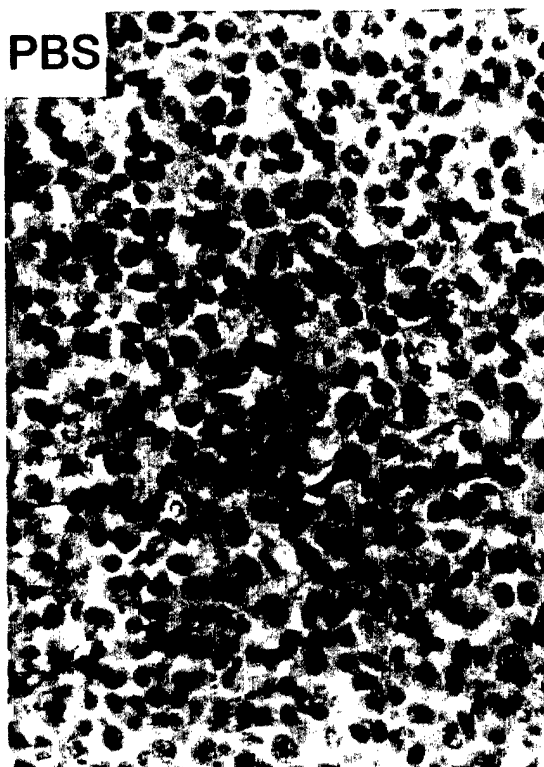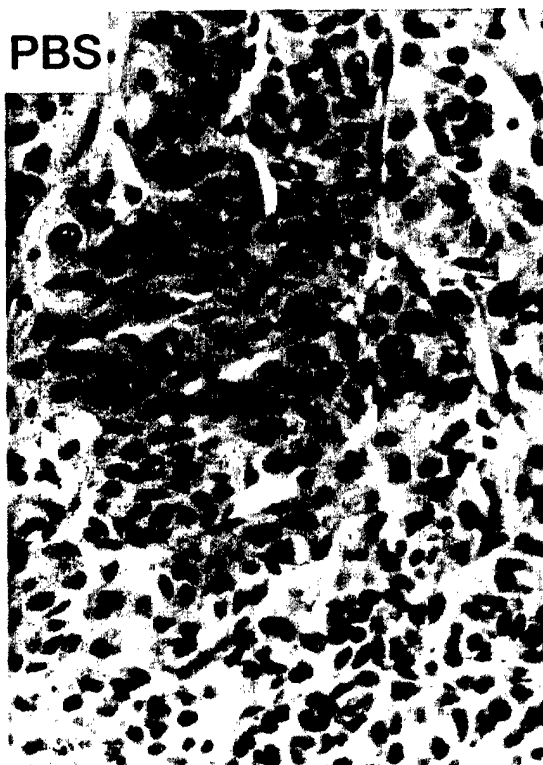
-saveLevel-
-mark-
-filestream-
-filestream-
1.00015
STACK:
OFFENDING COMMAND: image
ERROR: ioerror

A
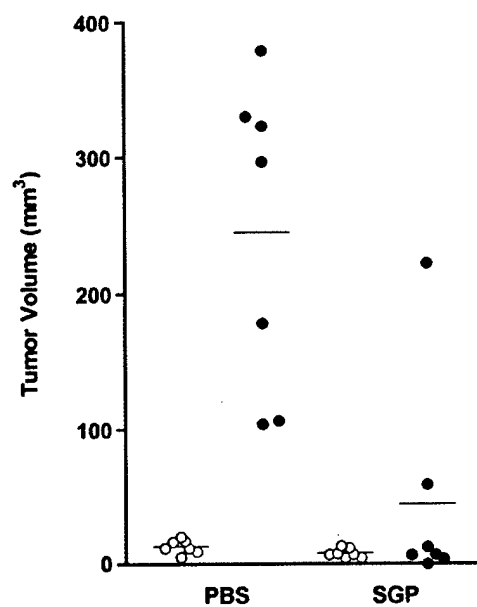
B
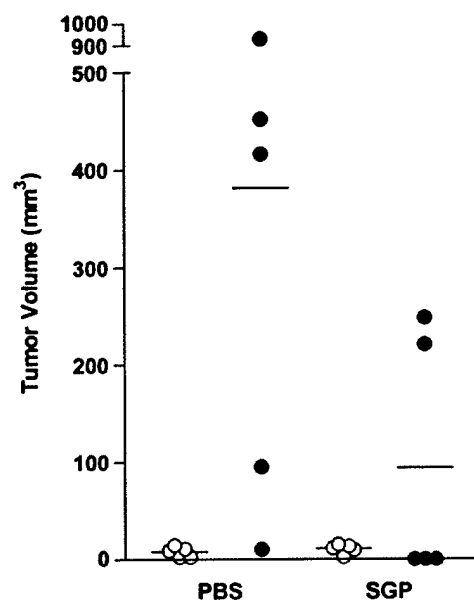
C
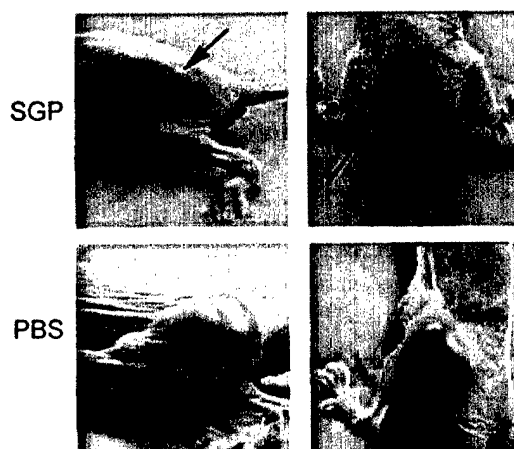
Cell Line	LC$_{50}$ at 30 min (μM)		
	SGP	SPG(L)	SPG(E)
KS 1767	5	60	30
MDA-MD-435	4	60	30
PC3	2.5	-	-
H-358	6	-	-
CADMEC	5	60	30
HUVEC	7	-	-
HPAEC	5	-	-
293	5	-	-

Cell Viability (%)

	Medium	Ethanol	Matrigel + Ethanol	SGP	Matrigel + SGP	sFn	sFN + SGP	FN + SGP
	+	−	−	−	−	−	−	−
	+	+	−	−	−	−	−	−
	+	−	+	−	−	−	−	−
	+	−	−	+	−	−	−	−
	+	−	−	−	+	−	−	−
	+	−	−	−	−	+	−	−
	+	−	−	−	−	−	+	−
	+	−	−	−	−	−	−	+

Cell Viability (%)

110

50

0

+	+	+	+	+	Medium
−	+	−	−	−	Dox
−	−	+	−	−	Matrigel + Dox
−	−	−	+	−	SGP
−	−	−	−	+	Matrigel + SGP

*